Forschungszentrum Karlsruhe
Technik und Umwelt

Wissenschaftliche Berichte
FZKA 6081

An Equation of State of Plutonium Nitride Fuel

E. A. Fischer

Institut für Neutronenphysik und Reaktortechnik
Projekt Nukleare Sicherheitsforschung

Mai 1998

Forschungszentrum Karlsruhe

Technik und Umwelt

Wissenschaftliche Berichte

FZKA 6081

An Equation of State of Plutonium Nitride Fuel

E. A. Fischer

Institut für Neutronenphysik und Reaktortechnik

Projekt Nukleare Sicherheitsforschung

Forschungszentrum Karlsruhe GmbH, Karlsruhe
1998

Als Manuskript gedruckt

Forschungszentrum Karlsruhe GmbH
Postfach 3640, 76021 Karlsruhe

Mitglied der Hermann von Helmholtz-Gemeinschaft
Deutscher Forschungszentren (HGF)

ISSN 0947-8620

Summary

An evaluation of the equation of state of plutonium nitride is presented. First, a simple anion defect model is applied to describe the evaporation behavior both of solid UN and PuN. It was found that the enormous pressure changes of both the metal vapor and nitrogen across the homogeneity range is representend in a satisfactory manner. Then, the extrapolation into the liquid range is carried out for PuN using a model which is based on an extension of the Significant Liquid Structures Theory. This model was developed earlier, in the context of evaluating the urania equation of state. At the present state of the art, significant data uncertainties and inconsistencies still exist, and the extrapolation to into the liquid range introduces further uncertainties. However, the present work produces results which are thermodynamically consistent, and in general agreement with the majority of measured data.

Eine Zustandsgleichung fuer Plutoniumnitrid

Zusammenfassung

Es wird eine Auswertung der Zustandsgleichung für Plutoniumnitrid vorgestellt. Zunächst wird ein einfaches Anionen-Defektmodell verwendet, um das Verdampfungsverhalten sowohl des festen UN als auch des PuN zu beschreiben. Das Verhalten der Drücke über den schmalen Homogenitätsbereich wird damit befriedigend wiedergegeben. Die Extrapolation in den Bereich des geschmolzenen PuN erfolgt mit Hilfe eines Modells, des auf einer Erweiterung der Significant Liquid Structures Theory beruht. Dieses Modell wurde bereits früher entwickelt, und auf die Erstellung der Zustandsgleichung von Urandioxid angewandt. Beim gegenwärtigen Kenntnisstand existieren noch viele Unsicherheiten und Inkonsistenzen in den verfügbaren Daten, die durch die Extrapolation in den flüssigen Bereich noch grösser werden. Jedoch sind die hier erstellten Daten thermodynamisch konsistent, und im allgemeinen mit den wichtigeren Messdaten verträglich.

An Equation of State of Plutonium Nitride Fuel

Contents

1 Introduction

In the frame of the CAPRA project, fast reactor designs are examined which can be used to burn plutonium and higher actinides. One option considered in these studies calls for nitride fuel, especially for plutonium nitride. The advantage, as compared to oxide fuel, is the better solubility of nitride, and its higher thermal conductivity. As the project involves also safety investigations, the equation of state of PuN is needed; in particular, the vapor pressure, which is the driving mechanism for shutdown in an energetic core disruptive accident. In the literature, vapor pressure data for nitride fuels were extrapolated above the melting point by Sheth and Leibowitz (1), and by Matsui and Ohse (2). Both authors used linear extrapolations of the log p versus 1/T data for the pressure of plutonium (or uranium) gas, and of nitrogen. This is overly simplistic. Besides, the change of slope at the melting point is not correct.

Ogawa, Ref (3), applied a sublattice formalism to describe the variation of the partial pressures across the homogeneity range. The quoted results are for solid nitrides only, but for the different fuels, UN, PuN, and mixed nitride. That work is very useful because it allows for a model description of the strong changes, and of the lower phase boundary.

In earlier work (4), the present author evaluated the equation of state of urania, which is representative of fast reactor oxide fuel, using an advanced method based on the Significant Structures Theory (SST) of liquids. The SST lends itself to an extension to non- stoichiometric systems. In that earlier work, the model parameters were fitted to experimental data, especially vapor pressure measurements over urania. In this work, the method developed in Ref (4) will be modified for nitride fuel, and used to evaluate the equation of state of PuN_{1-x} The method involves an anion point defect model. In a first step, this simple defect model will be applied to both solid UN and PuN up to the melting point. In a second step, the advanced method mentioned above will be used to extrapolate the data into the liquid range. This extrapolation is important for accident analysis. It will be carried out for the preferred nitride fuel, PuN, and used to produce equation of state data up to the critical point.

There are some experimental data, for vapor pressure and enthalpy (or specific heat), for UN, and still less for PuN. The vapor pressure measurements are typically within the range 1600 to 2300K. Therefore, the evaluation involves an enormous extrapolation, and large uncertainties. For some model parameters, only educated guesses are available. Nevertheless, it is

believed that this work is useful, for three reasons. First, it provides data which can be used in reactor accident analysis work. The present model includes more physics considerations than the earlier simplistic extrapolations, Ref (1,2), and therefore can be better defended than the earlier data. Second, the data are thermodynamically consistent. Third, the results allow to identify inconsistencies in the experimental data, and they convey a feeling of the limitations of this still rather simple and preliminary model. Also, they show where additional measurements are needed, in case the CAPRA project on the basis of PuN fuel progresses to the stage where accident analysis work is needed.

An evaluation of thermodynamic data was recently produced by Henshaw and Mignanelli, Ref (13). The goal of that work was to examine the thermal stability of Pu containig nitrides. The stability limit, at 2200K, was lower than the one suggested in the present evaluation.

2 Phase Diagram and Evaporation Processes for UN

The phase diagram of the U-N system, according to Tagawa (5), is shown in Fig.1. The part which is of interest for the present work is the rather narrow single-phase region UN_{1-x}, above about 1600K. The phase boundaries are not known accurately. We assume, following Ref (2), that the lower boundary is at N/U=0.96, and the upper boundary is close to, but still slightly below, unity. At the lower boundary, UN_{1-x} is in equilibrium with nitrogen-saturated liquid U. Observations indicate that both phases do not readily segregate. At the upper boundary UN_{1-x} is in equilibrium with a U_2N_3 phase. The melting point depends strongly on the nitrogen pressure, Ref (5). Congruent melting occurs at 3123K, see Ref (2), at a pressure of 2.5 atm. At lower pressures, the material decomposes into liquid uranium and nitrogen at temperatures below the congruent melting point. The homogeneity range, though very narrow, is characterized by large changes of both the uranium activity, and the nitrogen potential. It is one of the goals of this paper to test how well these changes can be described by a simple defect model. Evaporation of UN occurs, inside the homogeneity range, as a true evaporation process according to the reaction (Reaction 1)

$$UN_{1-x} = U(g) + \frac{1-x}{2} N_2 \qquad (1)$$

At the lower phase boundary, decomposition into nitrogen and liquid uranium occurs (Reaction 2) according to the equation

$$UN_{1-x} = U(l) + \frac{1-x}{2} N_2 \tag{2}$$

According to Ref (5,7), a congruently evaporating composition should exist at low enough temperatures. Potter (7) estimated that the limit is around 1700K, on the basis of theoretical arguments. This is, however, not consistent with certain literature data, which indicate a lower temperature limit. This will be discussed below. Here, it must be mentioned that above the limiting temperature, liquid uranium appears. This is because nitrogen evaporates faster than uranium in the homogeneity range, so that the sample composition changes toward lower N/U, until the phase boundary is reached. The condition for congruent evaporation in a Langmuir type experiment (where evaporation occurs essentially into vacuum) will be quoted here. It is a relation between the two partial pressures

$$\frac{p(U)}{p(N_2)} = 2\sqrt{\frac{M(U)}{M(N_2)}} \tag{3}$$

where the M's are the molecular weights.

In the reactor case, the available free volume is rather limited, and one has evaporation in a closed system, in which the overall composition changes very little. In such a closed system, a N/U exists where the total pressure is a minimum. This composition is sometimes also called "congruently evaporating", Ref (7). However, to avoid confusion, we will refer to "congruent evaporation" only in open systems.

The equilibrium constant, K, for Reaction 1, is defined by

$$K = p(U)\sqrt{p(N_2)} \tag{4}$$

and the free energy change in Reaction 1 is

$$\Delta G_T = -RT \ln K \tag{5}$$

The free energy change was determined from vapor pressure measurements by several authors; e.g. (6,8), assuming a linear dependence on temperature in a limited range. A complete list of references is given in (2). Matsui and Ohse, in their evaluation (2), recommend an equilibrium constant (or

free energy change) that is a weighted average over different published values. Note that the latter free energy change is connected to the thermal functions of the reaction partners by the equation

$$\Delta G_T = \Delta H_{298} - T\Delta(fef) \tag{6}$$

where H is the enthalpy, and fef the free energy function. $\Delta(H_{298})$ was determined e.g. by Gingerich (6). The free energy function of UN is tabulated in Ref (2), the one of U(g) in Ref (9) (we prefer this more recent work to the older IAEA tables), and the one of nitrogen in the JANAF tables, Ref (10). Therefore, the above equation allows a consistency check between vapor pressure data, and the thermal functions. The published values for the equilibrium constant for Reaction 1, as obtained from vapor pressure measurements, show a certain spread, which is larger than the one in the thermal functions. Therefore, it was decided to use the free energy change as given by the thermal functions, to define the slope of the vapor pressure curves. The absolute value, however, was taken from the equilibrium constant at 2100K (about at the center of the experimental data), as suggested by Matsui and Ohse (2). This determines the heat of reaction at 298K. The resulting value is close to the one found in Ref (6). In this sense, the data are consistent within their uncertainty range.

3 Equations of the Defect Model

The deviation from stoichiometry, though rather small, is important because both the uranium activity and the nitrogen potential show enormous changes. An earlier attempt to model this behavior was by Ogawa, Ref (3), who used a mixing model. In the present work, a simple anion point defect model will be applied to account for the deviation from stoichiometry. The model is similar to the one described in Ref (4), except that only anion vacancies are considered, not interstitials. This seems to be justified because there is evidence that the UN phase is always slightly substoichiometric. This model connects the absolute activity of nitrogen atoms, λ_N, to the density of vacancies. Note the following relation between λ_N and the nitrogen atom chemical potential, μ_N

$$\mu_N = RT \ln \lambda_N \tag{7}$$

Similar to Ref (4), the model is based on the following expression for the defect partition function, PF

$$PF = \sum \frac{N!}{N_v!(N-N_v)!} \exp\left(\frac{-N_v(\epsilon_v + \mu_N - N_v\epsilon_{vv}/N)}{kT} - N_v \ln q_v\right) \quad (8)$$

where N is Avogadro's number, N_v is the number of anion vacancies, and the sum is over N_v. This leads to the following relation between the relative vacancy concentration, $\Theta_v = Nv/N$, and the nitrogen activity

$$\ln \lambda_N = -\ln \frac{\Theta_v}{1-\Theta_v} - (\frac{\epsilon_v}{kT} + lnq_v) + 2\Theta_v \frac{\epsilon_{vv}}{kT} \quad (9)$$

Note that for the material UN_{1-x}, Θ_v is equal to x (in the absence of interstitials). In the above equation, ϵ_v is the energy required to remove a nitrogen lattice atom to infinity, ϵ_{vv} is the interaction energy between vacancies. The temperature θ_v corresponds to the energy of a typical lattice vibration, and the function q_v accounts for the vibrational modes associated with a missing lattice anion. It is given by

$$\ln(q_v(T)) = -3\left(\frac{\theta_v}{2T} + \ln\left(1 - \exp(-\frac{\theta_v}{T})\right)\right) - con \quad (10)$$

where con is a constant. The relation between the nitrogen potential, ΔG_{N2}, and the chemical potential μ_N, is

$$\Delta G_{N2} = 2\mu_N + D_0 + T(fef)_{N2,base0} \quad (11)$$

where D_0 is the dissociation energy of N_2. The free energy function fef, base 0, is related to the usual fef with base 298K, by

$$(fef)_{base0} = (fef)_{base298} - \frac{H_{298} - H_0}{T} \quad (12)$$

The Gibbs-Duhem equation in the single-phase range is

$$RTd\ln(p_U) + \frac{1-x}{2}d(\Delta G_{N2}) = 0 \quad (13)$$

Using equations (5,11), this can be rearranged to give

$$RTd\ln(K)_x = xRTd\ln\lambda_N \quad (14)$$

Combining this relation with eq (9), and integrating from x=0 to x leads to

$$\ln(K)_x - \ln(K)_{x\to 0} = \ln(1-x) + \frac{\epsilon_{vv}}{RT}x^2 \qquad (15)$$

According to the equations (7,9,11), the nitrogen potential goes to infinity for purely stoichiometric material, and so does the nitrogen pressure. This is a simplified mathematical description of the fact that, at the upper phase boundary, where N/U is still slightly less than unity, the nitrogen pressure is several orders of magnitude higher than at the lower phase boundary.

One finds easily that the uranium pressures at two compositions, x_1 and x_2, are related by

$$\ln\frac{p_{U,2}}{p_{U,1}} = \ln\frac{x_2}{x_1} + \frac{\epsilon_{vv}}{RT}(x_1 - x_2)(2 - x_1 - x_2) \qquad (16)$$

For congruent vaporization, the following relation must hold, see eq (3)

$$\frac{p_U}{p_{N2}} = 2\sqrt{\frac{M(U)}{M(N2)}} = 5.84 \qquad (17)$$

Using this condition, and assuming that the pressures at a point x_1 are given, one obtains the following equation for x_c, the composition for which congruent evaporation occurs

$$3\ln\frac{x_c}{x_1} = \ln\frac{p_{N2,1}}{p_{U,1}} + \ln\left(2\sqrt{\frac{M(U)}{M(N2)}}\right) + 2\ln\frac{1-x_c}{1-x_1} + W \qquad (18)$$

In this equation, W is

$$W = \frac{\epsilon_{vv}}{RT}(x_c - x_1)(6 - x_c - x_1) \qquad (19)$$

To connect these relations, which are based on the defect model, to the free energy change calculated from thermal functions, eq (6), we observe that the thermal functions of UN(s) are based on C_p measurements at lower temperatures, where the material is essentially stoichiometric. It seems, therefore, reasonable to assume that the fef, extrapolated to higher temperatures, refers also to nearly stoichiometric material. Thus, we have

$$\Delta(G_T, Reaction1) = -RT\ln(K)_{x\to 0} \qquad (20)$$

Then, combining this relation with eq (15) for x greater than zero gives

$$RT\ln(K)_x = -\Delta(G_T) + RT\ln(1-x) + \epsilon_{vv}x^2 \qquad (21)$$

While N_2 and U(g) are the two important species in the gas phase, Gingerich reports in Ref (6) that he has identified the UN(g) ion, by mass spectrometry, though with a very low intensity; about three orders of magnitude lower than U(g). He also quotes an estimated value, 60.7 kJ/mol, for the reaction enthalpy of the following Reaction 3

$$UN(g) = U(g) + 0.5N_2 \qquad (22)$$

at absolute zero. The parameters of the vapor pressure, based on Reactions 1 and 3, were estimated by Alexander (8), and by Matsui and Ohse (2). Both estimates are based on Gingerich's results. From these parameters, it is obvious that the pressure of UN(g) has a larger slope than the other partial pressures. Therefore, though the UN(g) pressure may be negligibly small around 2000K, it will become important at higher temperatures, and it must be included in a data extrapolation.

The free energy change of Reaction 3 is again given by eq (6), where the free energy of UN(g) must be estimated from the available data. The equilibrium constant is

$$K = \frac{p(U)\sqrt{p(N_2)}}{p(UN)} \qquad (23)$$

This completes the set of equations used to model the UN system in the solid range. The same equations are used for PuN.

4 Application to Solid UN

To apply the above model to the vaporization of UN, we use the equations (9,11,6,21). The following input data were taken from the literature: The free energy function of solid UN is tabulated in Ref (2), the one of U(g) in Ref (9), and the one of nitrogen in Ref (10). Ogawa (3) prepared the following analytic fit for the free energy of formation of gaseous U(g)

$$\Delta G_f(U_g) = 545590 - 343.952T + 27.002T\ln T \quad (J/mol) \qquad (24)$$

This fit is based on the tables in Ref (9). Equation (6) defines the temperature dependence of the equilibrium constant for Reaction 1, on the basis of the free energy functions, i.e. on the heat capacity data. The absolute

value depends also on the heat of reaction, ΔH_{298}, see eq (6). This quantity is chosen such that the vapor pressure values at 2100K, as recommended in Ref (2), are reproduced. This temperature was selected because it is about at the center of most experimental vapor pressure data points, see Ref (2), and especially Ref (6). One finds ΔH_{298} = 831930 J/mol, which is close to the value found by Gingerich, namely 838890 J/mol, from the Second Law of thermodynamics. Thus, the slope of the equilibrium constant is fairly well consistent with the Gingerich data. Alternatively, one could use the vapor pressure data to define the equilibrium constant as a function of temperature. However, there is a significant scatter between the different measurements, so we prefer the method just described. The nitrogen pressure as a function of T and x is then obtained from the defect model. The input values which seem to give the best fit to experimental data are

$$\epsilon_v = 790340\, J/mol \qquad \epsilon_{vv} = 50292\, J/mol$$
$$con = -0.4999 \qquad \theta_v = 540K$$

Note that the vapor pressure data refer to the lower phase boundary, which is taken as x=0.04 at 2100K, see Ref (2,3). Further, we observe that the uranium activity at 2100K is a_U = 0.391, according to the literature data used. It is then assumed that a_U increases linearly with temperature, up to the melting point. The slope is chosen such that the partial pressures converge towards lower temperatures, in a similar manner as the evaluation in Ref (2). a_U at the melting point is chosen as 0.53, which gives reasonable results.

Fig.2 shows the two partial pressures of N_2 and U(g) at the lower phase boundary. They compare well with literature data. Fig.3 shows the pressures at 2000K across the single-phase region. This is comparable to Ogawa's results, Ref (3). The lower phase boundary as a function of temperature is shown in Fig.4. It is nearly constant, in agreement with Ref (2,3). These results show that the present model is suitable to describe the vaporization behavior of UN, at least in an approximate way. One could even argue that the use of a more complex model is not justified in view of the currently existing uncertainties of the experimental data.

Note that with the data chosen, the U pressure is lower than the nitrogen pressure over the temperature range of interest, so that the model does not predict congruent vaporization, down to 1600K. This result does not agree with the findings by Potter (7).

It is interesting in this context to look at the partial pressures at the lower and the upper phase boundary at a certain temperature, e.g. 1600K, for which a plot across the single-phase region is shown in Ref (2). We first look at the lower phase boundary, to which the above vapor pressure data refer. The U pressure is obviously given by

$$RT \ln p_U = -\Delta G_f(U(g)) + RT \ln a_U \tag{25}$$

whereas, according to the partial reaction,

$$UN(s) = U(l) + 0.5N_2 \tag{26}$$

the pressure of N_2 is given by

$$0.5RT \ln p_{N2} = \Delta G_f(UN) - RT \ln a_U \tag{27}$$

After inserting data into the above equations, we find

$$\log p_{N2} = -10.712 - 2 \log a_U$$

$$\log p_U = -10.251 + \log a_U$$

where the pressure is in atmospheres, and log refers to base 10. The vapor pressure data, Ref (2), indicate that the uranium activity is less than unity, of the order of 0.3. Therefore, the U pressure is nearly one order of magnitude lower than the N_2 pressure, so that no minimum of the total pressure across the single-phase region exists. It is important to note that this conclusion is based on very few literature data, namely the two free energies of formation of U(g) and UN, and the observation that a_U is of the order of 0.3. Clearly, the conclusion contradicts the statements by Potter (7) that UN vaporizes congruently up to 1700K. This illustrates that there are still significant inconsistencies and uncertainties in the data.

Let us now look at the upper phase boundary, between UN and $UN_{1.5}$. Matsui and Ohse use an equation proposed by Tagawa (5) to find the nitrogen pressure at 1600K, $logp_{N2} = -0.136$. To obtain the U pressure, they use the equilibrium of the reaction

$$3UN = U(g) + 2UN_{1.5}$$

where the free energy of formation of $UN_{1.5}$ is again given by Tagawa. This leads to $logp_U = -26.2$. First, there is an enormous change of the partial pressures across the single-phase region, but this is to be expected. The

nitrogen pressure increases by about 10 decades, the U pressure decreases by about 15 decades. This, however, is not consistent with the Gibbs-Duhem relation, eq (13) or (14). As x is small, the change in log p(U) must be about half the change in log p(N2). Thus, at least one of the values at the upper phase boundary is grossly in error. Assume for the moment that the nitrogen pressure is more reliable. Then, log p(U) should be of the order -16. A more accurate estimate can be produced by applying the defect model. At 1600K, the nitrogen pressure suggested by Tagawa is reached for x=3.1E-07. Then, using eq (16) with x=0.04 at the lower phase boundary, one finds

$$\log p_U = -15.76$$

at the upper phase boundary. This result reflects the fact that the defect model is consistent with the Gibbs-Duhem relation, as must be.

It remains to evaluate the pressure of UN(g), based on Reaction 3, equations (22,23). There are no experimental data on UN(g), but vapor pressure curves were estimated in Ref (2) and (8). We use the vapor pressure equation from Ref (2) to obtain the enthalpy and entropy of UN(g) at 2100K. The specific heat C_p is estimated by comparison with other diatomic gases to be 48.1 J/molK. The resulting vapor pressure curve is shown in Fig.5. Note that in Ref (2), the linear log K vs. 1/T assumption implies that ΔC_p of the reaction is zero. Our approximation, with constant C_p of UN(g), is in principle more accurate, but there is clearly a large uncertainty in the latter quantity.

In summary, it appears that the present model provides a valid description of the vaporization behavior of UN. Especially, the thermal data of the components lead to vapor pressure curves which are within the range of direct vapor pressure measurements. Clearly, there is some arbitrariness in the choice of the model parameters, especially the U activity at the melting point. The exact choice depends, however, on the weight the evaluator assigns to different experimental data. It must be emphasized again that significant data uncertainties still exist.

5 Application to Solid PuN

The evaluation of the PuN data proceeds in general along the same lines as that of UN, and the same equations are used. Again, the free energy function of solid PuN is taken from Ref (2), and the one of Pu(g) from Ref (9). The

free energy of formation of gaseous Pu is approximated by an analytic fit, which was prepared using the tables in Ref (9)

$$\Delta G_f(Pu_g) = 324632 - 84.40T - 0.001988T^2 \quad (J/mol) \qquad (28)$$

It was, however, found that the thermal data, i.e. the free energy functions, and the vapor pressure data are not as well consistent as those for UN. If the tabulated free energy functions are used, through the eqs (6,21), to produce vapor pressure curves, then these differ slightly from the direct measurements by Kent and Leary, Ref (11). Ogawa, in his evaluation, Ref (3), adjusted his model parameters to the vapor pressure data, and did not use the thermal data at all. However, in the present work, the goal is to produce data which are thermodynamically consistent. Therefore, an ad hoc procedure was used. First, it was observed that the pressure of gaseous Pu, as measured by Kent and Leary, Ref (11), Alexander et al, Ref (2), and Suzuki et al, Ref (12), agree within reasonable limits (about 25 percent). Second, the heat of Reaction 1 can be found by combining the enthalpy of formation of PuN, which is 299.2 kJ/mol, Ref (2), with the heat of vaporization of Pu which is 349.0 kJ/mol, Ref (9). Both add up to 648.2 kJ/mole. Combining this with the thermal functions of the reaction partners, one can calculate the pressure of Pu(g). Around 1800K, which is the average temperature of Kent and Leary's data, the pressure shows the correct slope, but is too low. Thus, in our ad hoc procedure, the entropy of PuN was artificially increased by 8.368 J/molK, as compared to the tabulated values in Ref (2), in order to raise the calculated pressure to the measured value. In addition, a slight adjustment of the reaction enthalpy was carried out using the data of Ref (11). The result is $\Delta H_{298} = 646.18$ kJ/mol, which differs only slightly from the above value, 648.2 kJ/mol.

For PuN, the condition for congruent vaporization, eq (17), is fulfilled up to temperatures well above 2000K. Following Kent and Leary, it is assumed that the N/Pu corresponding to congruent vaporization at 1800K is 0.98. It follows from the vapor pressure data that the Pu activity at this point is 0.118. The activity at the lower phase boundary is assumed to be 0.5, which is slightly lower than the estimate by Kent and Leary, 0.6. The activity at the lower phase boundary increases with temperature, and a linear increase is assumed, similar to UN. At the melting point, the activity is taken to be 0.8. Again, there is some arbitrariness, but these values give satisfactory results. The input values of the defect model were chosen as follows

$$\epsilon_v = 709538\, J/mol \qquad \epsilon_{vv} = 0$$
$$con = -4.8552 \qquad \theta_v = 540K$$

Fig.6 shows the composition where vaporization is congruent, and the lower phase boundary (LPB). The former increases only slightly, which is consistent with Kent and Leary, and with Ogawa. The latter decreases with temperature, but is generally lower than Ogawa's LPB. Both curves intersect at 2687K. Below this temperature, congruent vaporization occurs, and the corresponding N/Pu is an equilibrium composition. Above the limiting temperature, the calculated congruent vaporizing composition lies outside the single-phase range and, therefore, becomes meaningless. Instead, the vaporizing material approaches the LPB, where it is in equilibrium with nitrogen saturated liquid Pu. This means that liqiud Pu metal appears above the limiting temperature.

The value found for this temperature is in reasonable agreement with the findings reported by Kent and Leary. It is, however, higher than the value of 2200K, which was suggested in the evaluation by Henshaw and Mignanelli, Ref (13). This difference reflects uncertainties and inconsistencies in the available data, which are larger for PuN than for UN. In our present evaluation, the model parameters were adjusted to the vapor pressure data by Kent and Leary, Ref (11), and to the thermal data by Matsui and Ohse, Ref (2). Furthermore, the results are consistent with the data by Alexander et al, see Ref (2).

Fig.7 shows the pressures of nitrogen and Pu(g). At congruent vaporization, both pressures differ by the constant factor 5.84, see eq (17). As mentioned, these pressures are valid below the limiting temperature, 2687K. Above 2687K, the pressures at the LPB are valid; they are also shown in the Figure. Obviously, both vapor pressure curves change slope at 2687K, and the straight-line extrapolations of the type quoted by Matsui and Ohse (2) are no longer meaningful above this temperature. Only the equilibrium constant of Reaction 1 can still be compared.

To evaluate the PuN(g) pressure, we used the estimated curve of Ref (2), in a similar way as for UN(g). For the specific heat of PuN(g), the same value as for UN(g), 48.1 J/mol-K, was used. The result is shown in Fig.8. Note that the PuN(g) pressure depends only weakly on the composition variable x. Therefore, it was evaluated only for the congruently vaporizing composition.

As seen in Fig.9, the partial pressures at 2000K, as functions of N/Pu, behave in a similar manner as the pressures above UN, except that the Pu pressure is much higher than the U pressure, and of the same order as the N_2 pressure. Therefore, congruent vaporization of PuN is possible.

The present model, with the artifact of an increased entropy of PuN, produces reasonable and consistent data at congruent vaporization. Note that Kent and Leary (11) quote also measured pressure data of Pu(g) at the LPB, at temperatures around 1600K. These data are probably not as reliable as those at congruent vaporization. Our evaluation is roughly consistent with them, in the sense that Kent and Leary quote 0.6 for the Pu activity, whereas our value at 1600K is 0.45. This is different from Ogawa (3), who assumes that the Pu activity at the LPB is equal to unity over the whole temperature range examined. In the present evaluation, x at the LPB decreases rather strongly from 0.14 a 1600K to about 0.021 at the melting point. This does not contradict any experimental information, though it is different from Ogawa, who assumes that x is constant.

6 Equation of State: The Grand Partition Function

The present equation of state model starts from a Grand Partition Function (GPF) for PuN_{1-x}. We deal with one mol nitride, i.e. one mol of Pu, but the number of nitrogen atoms is determined by the nitrogen chemical potential. Strictly, the system is described by a semi-grand partition function. The formalism was developed in Ref (4) for urania. For nitride, the equations are somewhat simpler because only substoichiometric material is treated.

The (semi-)grand PF can be written

$$GPF(T, V, \mu_N) = \sum \exp(\frac{\mu_N N_N}{kT}) Z(T, V, N_N) \tag{29}$$

where Z is the usual canonical PF for one mol of PuN_{1-x}, with a given value of x. The sum is over N_N, the number of anion sites occupied by a nitrogen ion. Note that $1 - x = N_N/N$, where N is Avogadro's number, and V is the molar volume. The thermodynamic potential corresponding to this GPF is

$$J(T, V, \mu_N) = -kT \ln(GPF) \tag{30}$$

It is equal to

$$J = U - S - \mu_N N_N \tag{31}$$

where U is the internal energy, and S the entropy. Its differential is

$$dJ = -SdT - pdV - N_N d\mu_N \tag{32}$$

To proceed further, we introduce now the equations of the Significant Structures Theory (SST) of liquids, see e.g. Ref (4). The basic assumption is that the PF of the liquid is composed of a solidlike part, f_s, and a gaslike part, f_g. Thus, one has

$$\ln Z = N\frac{V_s}{V}\ln f_s(T,V,N_N) + N\frac{V-V_s}{V}\ln f_g(T,V,N_N) \tag{33}$$

where V_s is the molar volume of the solid material at the melting point.

We now introduce N_b, the number of nitrogen vacancies per mol of PuN_{1-x}, through the relations

$$N_N = N - N_b \qquad N_b = xN \tag{34}$$

and observe that the factor in eq (29) which includes N in the exponential function can be omitted by a change in normalization. The grand partition function is then

$$GPF = \sum \exp(\frac{-\mu_N N_b}{kT}) Z(T,V,N_b) \tag{35}$$

It is known from statistical thermodynamics that a sum of this type can be approximated by its maximum term. If N_{bm} is the value of N_b which belongs to the maximum term, one obtains, using eq (33)

$$\ln(GPF) = N\frac{V_s}{V}\ln f_s + N\frac{V-V_s}{V}\ln f_g - \frac{\mu_N N_{bm}}{kT} \tag{36}$$

The solidlike PF is composed of the PF for the perfect lattice, $f_{s0}(T,V)$, and of a defect PF, lnZ_{def}, which accounts for the influence of the anion point defects, see Section 3. Similarly, the gaslike PF is composed of a "stoichiometric" part f_{g0} (i.e. for gaseous PuN), and a part Z_{gn}, which accounts for gaseous Pu, i.e., the nonstoichiometric component. The equations are derived in the Appendix. Therefore, we have

$$\ln f_s = \ln f_{s0} + \ln Z_{def} \tag{37}$$

$$\ln f_g = \ln f_{g0} + \ln Z_{gn} \tag{38}$$

The PF for the perfect lattice is taken from the SST. It reads

$$\ln f_{s0} = 2(x_1 - x_2 + x_3) \tag{39}$$

where x_1, x_2, x_3 are given by

$$x_1 = \frac{E_s}{2RT}(\frac{V}{V_s})^\gamma \tag{40}$$

$$x_2 = 3\ln\left(1 - exp(-\frac{\theta_E}{T})\right) \tag{41}$$

$$x_3 = \ln\left(1 + n\frac{V - V_s}{V_s}\exp(-\frac{aV_s x_1}{V - V_s})\right) \tag{42}$$

These are the same expressions that were used in earlier work, except that they are now written for a diatomic compound.

The variables are:

E_s binding energy of the PuN crystal

Θ_E Einstein temperature of the lattice vibrations

a, n, γ model parameters

The defect PF, which accounts for the effect of the anion vacancies, is according to Section 3

$$ln(Z_{def}) = -xlnx - (1-x)ln(1-x) - x(\frac{\epsilon_v}{kT} + \ln q_v) + \frac{\epsilon_{vv}}{kT}x^2 \tag{43}$$

Similarly, the gaslike PF can be split into a "stoichiometric" part, which is simply the PF of PuN(g), see the Appendix

$$\ln(f_{g0}) = \ln\frac{f_1 eV}{N} \tag{44}$$

where f_1 is the temperature dependent part of the PF for PuN(g), and e the base of the natural logarithm. The second part, which describes the deviation from stoichiometry, is according to the Appendix

$$\ln(Z_{gm}) = x\ln\frac{f_0}{f_1} - x\ln x - (1-x)\ln(1-x) \tag{45}$$

In this expression, f_0 is the temperature dependent part of the PF of Pu(g); the latter causes the N/Pu to be much lower than unity in the gas phase. The second and third terms in the above equation account for the mixing entropy of the gas.

After inserting these different expressions into the equation for the GPF, one finds that the part which depends on x is (omitting the factor N)

$$\ln(GPF(x)) = \frac{V_s}{V}\ln(Z_{def}) + \frac{V - V_s}{V}\ln(Z_{gm}) \qquad (46)$$

Remember now that the value of x to be used in this equation is the one for which the above expression is a maximum. Therefore, the derivative with respect to x must be zero. This gives the condition

$$\ln\frac{1-x}{x} - \frac{\mu_N}{kT} - \frac{V_s}{V}\left(\frac{\epsilon_v}{kT} + \ln q_v - 2x\frac{\epsilon_{vv}}{kT}\right) - \frac{V - V_s}{V}\ln\frac{f_1}{f_0} = 0 \qquad (47)$$

This completes the equations which are used to extrapolate the PuN equation of state into the liquid range. A more detailed derivation and discussion is given in Ref (4).

7 Equation of State of PuN above the Melting Point

The evaluation of the equation of state of PuN was carried out using the formalism described in Section 6, which is based on an extension of the Significant Structures Theory of liquids. The model parameters were chosen from the following criteria: At the melting point, the PuN(g) pressure is the same as for solid material. The liquid specific volume is not known. The value used in the model was found assuming a volume increase of 10 percent upon melting, which is similar to urania. Along the same line, the volumetric expansion coefficient was assumed around 1.0E-04, again as for urania. The vapor pressure slope versus temperature is determined from the heat of vaporization, which is the heat of sublimation in the solid, minus the heat of fusion, taken from Ref (2). The parameters for which the results satisfy these criteria are

$$E_s = 594130\,J/mol \qquad \Theta_E = 113.8K \qquad a = 0.003$$
$$n = 10.5 \qquad \gamma = 0.057 \qquad 1/V_s = 12992\,kg/m^3$$

To assure consistency, the same data as for solid PuN were used for the defect model. At the triple point, solid and liquid are in equilibrium. Therefore, the Pu activity has the same value as in the solid, namely 0.8.

The model then predicts an x of 0.036 at the LPB, somewhat larger than in the solid. Model calculations show that x will increase with temperature. To limit this increase, a decrease of the Pu activity was assumed, taking the value 0.53 at 7500K. Clearly, this assumption is based only on engineering judgement.

The results will now be discussed. In the liquid range, there is no congruent vaporization, just as there is none in the solid close to the melting point. Thus, for free vaporization, the lower phase boundary (LPB) is the only equilibrium point at any temperature. The LPB is shown in Fig.10. First, N/Pu decreases slightly with temperature, which seems reasonable. Then, as the critical point is approached, the decrease becomes stronger, so that the value N/Pu=0.795 is reached at the critical point. This is the same value as in the gas phase, as must be.

The pressures of Pu(g) and PuN(g) at the LPB are shown in Fig.11. It is obvious that the PuN(g) pressure becomes dominant at higher temperatures, above about 4500K. Interestingly, the Pu(g) pressure decreases in the vicinity of the critical point. The reason is that N/Pu must then be equal in the liquid and the gas phase, as mentioned before. Fig.12 shows the saturation pressure, which is defined as the total of the two Pu-bearing species, Pu and PuN. The total pressure, which includes the nitrogen contribution, is also shown. These pressures, which correspond to a stable configuration, namely the LPB, should be used in accident analysis calculations.

Fig.13 presents the liquid and the saturated vapor densities at the LPB, up to the critical temperature. The shape of the liquid density function is as expected: Directly above the melting point, the decrease is nearly linear, but with a slight downward curvature. The curvature becomes larger as the critical point as approached. The law of rectilinear diameter is fulfilled in good approximation.

The specific heats and some other quantities at the melting point are

$$C_v = 194\,J/kgK \qquad C_p = 350\,J/kgK$$
$$\alpha = 0.965E-04\,(1/K) \qquad \beta = 1.53E-05\,(1/Mpa)$$
$$\rho = 11720\,kg/m^3 \qquad T_m = 3000K$$

where alpha is the volumetric expansion coefficient, and beta the (isothermal) compressibility. These data fulfill the relation

$$C_p = C_v + \frac{T_m \alpha^2}{\rho \beta} \tag{48}$$

The extrapolation of the liquid specific enthalpy (at the LPB) is shown in Fig.14.

The partial pressures were obtained for different N/Pu values. To demonstrate the dependence on the x variable, some results are shown in the attached Tables. The values at the LPB are also shown.

The critical temperature depends on N/Pu. However, the important point is again the LPB, and the corresponding data will be quoted. The model predicts a critical temperature of 7480K, and a critical density of $2400 kg/m^3$. The critical saturation pressure is 168 Mpa, the corresponding total pressure (including nitrogen) is 203 Mpa. These data give a critical compressibility of 0.285, which is within the expected range. It is interesting that the critical temperature is lower than for urania, while the critical pressure is comparable. The main reason is that the predicted PuN pressure has a larger slope than the one of UO_2 above urania. Here, the weakest point in the whole extrapolation must be mentioned: The data of PuN(g) are only assessed on theoretical arguments, whereas the species has not even been identified in the experiments. In general, there are only few experimental data, so that the EOS evaluation involves extrapolations and estimates, so there are large uncertainties.

8 Conclusions

It was shown that the thermodynamic properties (partial pressures, enthalpy) of solid UN and PuN can be interpreted in terms of a simple anion defect model. Especially, the dependence of the partial pressures on N/M (M is U or Pu) was predicted in a satisfactory way. The gas species considered are M(g), nitrogen, and MN(g). Furthermore, the equation of state of substoichiometric PuN was evaluated, starting from a formulation with a grand partition function. For further evaluation, a modified version of the Significant Structures Theory of liquids was applied. As there are only few experimental data available for PuN, large uncertainties exist. It is, however, believed that the present evaluation is useful, because the results look reasonable, and are, in general, compatible with the - scarce - experimental information, and because the formalism is thermodynamically consistent. Thus, the results deserve more confidence than previous simple extrapolations, which do not have the latter property.

If ever more reliable data are required, then additional experiments must be carried out. It is necessary to extend the temperature range of the vapor

pressure measurements, to identify and study the PuN molecule, and to produce some data (density, thermal expansion) for molten PuN.

9 References

1. A. Sheth and L. Leibowitz
   Report ANL-AFP-12 (1975)
2. T. Matsui and R. W. Ohse
   High Temperatures-High Pressures 19, 1 (1987)
3. T. Ogawa
   J. Nucl. Mater. 201, 284 (1993)
4. E.A. Fischer
   Report KfK-4084 and Nucl. Sci. Eng. 101, 97 (1989)
5. H. Tagawa
   J. Nucl. Mater. 51, 78 (1974)
6. K.A. Gingerich
   J. Chem. Phys. 51, 4433 (1969)
7. P.E. Potter
   J. Nucl. Mater. 47, 7 (1973)
8. C.A. Alexander et al.
   J. Nucl. Mater. 31, 13 (1969)
9. E.H.P. Cordfunke and R.J.M. Konings
   Thermodynamic Data for Reactor Materials and Fission Products
   North Holland Publishing Company, Amsterdam 1990
10. National Bureau of Standards
    JANAF Thermochemical Tables (1971)
11. R.A. Kent and J. A. Leary
    High Temp. Sci. 1, 176 (1968)
12. R.A. Suzuki et al
    J. Nucl. Mater. 51, 78 (1974)
13. J. Henshaw and M.A. Mignanelli
    The thermal stability of nitride fuel
    Commercial report of AEA Technology, 1996

10 Appendix: The PF of the Gas Mixture

To develop the equation of state formalism to be used in this work, the partition function of the gas mixture is needed. The Pu-bearing gas species considered are Pu(g) and PuN(g). They are in equilibrium with N_2 through the nitrogen chemical potential. Though PuN(g) is unimportant at temperatures at or around 2000K, it is predicted to contribute significantly to the vapor pressure above the liquid, and thus it must be included in the model. Let the subscript 0 indicate Pu(g), and the subscipt 1 stand for PuN(g). Then the gas PF for one mol of mixture is

$$\ln(Z_{gas}) = N_0 \ln \frac{f_0 eV}{N_0} + N_1 \ln \frac{f_1 eV}{N_1} \tag{49}$$

If x means the fraction of missing N atoms as compared to stoichiometric gas then the relations hold

$$N_0 + N_1 = N \qquad N_0 = xN \tag{50}$$

and the above equation can be written, after some simple manipulations

$$\ln(Z_{gas}) = N \left(\ln \frac{f_1 eV}{N} + x \ln \frac{f_0}{f_1} - x \ln x - (1-x)\ln(1-x) \right) . \tag{51}$$

We now notice that the first term is simply the PF of PuN(g), i.e. for stoichiometric vaporization; we denote this by f_{g0},

$$\ln(f_{g0}) = \ln \frac{f_1 eV}{N} \tag{52}$$

and the other terms account for the deviation from stoichiometry. Denote them Z_{gn}, so that

$$\ln(Z_{gn}) = x \ln \frac{f_0}{f_1} - x \ln x - (1-x)\ln(1-x) \tag{53}$$

These are the expressions used in the present model for the gas PF.

TABLE I: PARTIAL PRESSURES (MPA) ABOVE PUN, N/PU= 0.970

TEMP	X(GAS)	P(PU)	P(PUN)	PSAT	P(N2)	PTOT
3000.0	0.841	7.6683E-03	1.4445E-03	9.1128E-03	4.7818E-03	1.3895E-02
3500.0	0.645	5.2454E-02	2.8925E-02	8.1379E-02	7.0656E-02	1.5204E-01
4000.0	0.462	2.1332E-01	2.4856E-01	4.6188E-01	5.3016E-01	9.9204E-01
4500.0	0.331	6.1065E-01	1.2314E+00	1.8421E+00	2.6157E+00	4.4578E+00
5000.0	0.243	1.3511E+00	4.1982E+00	5.5493E+00	9.7919E+00	1.5341E+01
5500.0	0.183	2.4759E+00	1.1022E+01	1.3498E+01	3.0426E+01	4.3924E+01
6000.0	0.141	3.9373E+00	2.3988E+01	2.7926E+01	8.3428E+01	1.1135E+02
6500.0	0.109	5.5363E+00	4.5487E+01	5.1023E+01	2.1133E+02	2.6235E+02
7000.0	0.082	6.9314E+00	7.7750E+01	8.4681E+01	5.1588E+02	6.0056E+02
7250.0	0.070	7.3797E+00	9.8525E+01	1.0590E+02	8.0860E+02	9.1451E+02
7375.0	0.064	7.4933E+00	1.1017E+02	1.1767E+02	1.0184E+03	1.1360E+03
7500.0	0.058	7.5016E+00	1.2271E+02	1.3021E+02	1.2929E+03	1.4231E+03
7750.0	0.044	6.9821E+00	1.5044E+02	1.5742E+02	2.2039E+03	2.3614E+03

TABLE II: PARTIAL PRESSURES (MPA) ABOVE PUN, N/PU= 0.940

TEMP	X(GAS)	P(PU)	P(PUN)	PSAT	P(N2)	PTOT
3000.0	0.916	1.5201E-02	1.4008E-03	1.6602E-02	1.1547E-03	1.7757E-02
3500.0	0.787	1.0392E-01	2.8081E-02	1.3200E-01	1.7031E-02	1.4903E-01
4000.0	0.637	4.2357E-01	2.4185E-01	6.6542E-01	1.2791E-01	7.9334E-01
4500.0	0.501	1.2091E+00	1.2027E+00	2.4118E+00	6.3282E-01	3.0446E+00
5000.0	0.394	2.6841E+00	4.1200E+00	6.8041E+00	2.3770E+00	9.1811E+00
5500.0	0.311	4.9175E+00	1.0879E+01	1.5796E+01	7.4212E+00	2.3217E+01
6000.0	0.248	7.8511E+00	2.3821E+01	3.1672E+01	2.0449E+01	5.2121E+01
6500.0	0.195	1.1032E+01	4.5458E+01	5.6490E+01	5.2184E+01	1.0867E+02
7000.0	0.150	1.3750E+01	7.8201E+01	9.1951E+01	1.2879E+02	2.2074E+02
7250.0	0.128	1.4560E+01	9.9440E+01	1.1400E+02	2.0359E+02	3.1759E+02
7375.0	0.117	1.4716E+01	1.1139E+02	1.2611E+02	2.5798E+02	3.8409E+02
7500.0	0.105	1.4626E+01	1.2427E+02	1.3889E+02	3.3038E+02	4.6927E+02
7750.0	0.079	1.3050E+01	1.5301E+02	1.6606E+02	5.8927E+02	7.5533E+02

TABLE III: PARTIAL PRESSURES (MPA) ABOVE PUN, N/PU= 0.910

TEMP	X(GAS)	P(PU)	P(PUN)	PSAT	P(N2)	PTOT
3000.0	0.943	2.2411E-02	1.3585E-03	2.3770E-02	4.9450E-04	2.4264E-02
3500.0	0.850	1.5446E-01	2.7240E-02	1.8170E-01	7.2843E-03	1.8899E-01
4000.0	0.728	6.3079E-01	2.3509E-01	8.6588E-01	5.4784E-02	9.2067E-01
4500.0	0.605	1.7956E+00	1.1737E+00	2.9693E+00	2.7170E-01	3.2410E+00
5000.0	0.497	3.9996E+00	4.0399E+00	8.0395E+00	1.0242E+00	9.0637E+00
5500.0	0.407	7.3522E+00	1.0728E+01	1.8080E+01	3.2097E+00	2.1290E+01
6000.0	0.332	1.1738E+01	2.3640E+01	3.5378E+01	8.9020E+00	4.4280E+01
6500.0	0.266	1.6484E+01	4.5417E+01	6.1900E+01	2.2893E+01	8.4793E+01
7000.0	0.206	2.0447E+01	7.8684E+01	9.9131E+01	5.7166E+01	1.5630E+02
7250.0	0.176	2.1512E+01	1.0042E+02	1.2193E+02	9.1245E+01	2.1317E+02
7375.0	0.161	2.1620E+01	1.1269E+02	1.3431E+02	1.1645E+02	2.5076E+02
7500.0	0.145	2.1291E+01	1.2596E+02	1.4725E+02	1.5071E+02	2.9796E+02
7625.0	0.126	2.0259E+01	1.4033E+02	1.6059E+02	2.0061E+02	3.6120E+02

TABLE IV: PARTIAL PRESSURES (MPA) ABOVE PUN, N/PU= 0.880

TEMP	X(GAS)	P(PU)	P(PUN)	PSAT	P(N2)	PTOT
3000.0	0.958	2.9637E-02	1.3154E-03	3.0953E-02	2.6763E-04	3.1220E-02
3500.0	0.885	2.0407E-01	2.6401E-02	2.3047E-01	3.9368E-03	2.3441E-01
4000.0	0.784	8.3026E-01	2.2847E-01	1.0587E+00	2.9655E-02	1.0884E+00
4500.0	0.676	2.3821E+00	1.1441E+00	3.5262E+00	1.4737E-01	3.6736E+00
5000.0	0.572	5.2987E+00	3.9580E+00	9.2567E+00	5.5774E-01	9.8144E+00
5500.0	0.479	9.7393E+00	1.0575E+01	2.0314E+01	1.7616E+00	2.2076E+01
6000.0	0.399	1.5598E+01	2.3449E+01	3.9047E+01	4.8994E+00	4.3946E+01
6500.0	0.325	2.1887E+01	4.5367E+01	6.7254E+01	1.2702E+01	7.9956E+01
7000.0	0.254	2.7003E+01	7.9186E+01	1.0619E+02	3.2120E+01	1.3831E+02
7250.0	0.217	2.8198E+01	1.0146E+02	1.2966E+02	5.1834E+01	1.8150E+02
7375.0	0.198	2.8141E+01	1.1411E+02	1.4226E+02	6.6718E+01	2.0897E+02
7500.0	0.176	2.7368E+01	1.2786E+02	1.5523E+02	8.7603E+01	2.4283E+02
7625.0	0.150	2.5265E+01	1.4281E+02	1.6807E+02	1.2059E+02	2.8866E+02

TABLE V: PARTIAL PRESSURES (MPA) ABOVE PUN, N/PU= 0.850

TEMP	X(GAS)	P(PU)	P(PUN)	PSAT	P(N2)	PTOT
3000.0	0.966	3.6461E-02	1.2742E-03	3.7735E-02	1.6446E-04	3.7900E-02
3500.0	0.908	2.5111E-01	2.5594E-02	2.7670E-01	2.4159E-03	2.7912E-01
4000.0	0.822	1.0249E+00	2.2188E-01	1.2468E+00	1.8233E-02	1.2650E+00
4500.0	0.726	2.9485E+00	1.1147E+00	4.0632E+00	9.0859E-02	4.1541E+00
5000.0	0.629	6.5802E+00	3.8748E+00	1.0455E+01	3.4491E-01	1.0800E+01
5500.0	0.537	1.2099E+01	1.0416E+01	2.2515E+01	1.0991E+00	2.3614E+01
6000.0	0.455	1.9430E+01	2.3248E+01	4.2677E+01	3.0645E+00	4.5742E+01
6500.0	0.376	2.7248E+01	4.5303E+01	7.2551E+01	8.0125E+00	8.0564E+01
7000.0	0.295	3.3406E+01	7.9724E+01	1.1313E+02	2.0539E+01	1.3367E+02
7250.0	0.252	3.4620E+01	1.0255E+02	1.3717E+02	3.3567E+01	1.7073E+02
7375.0	0.228	3.4191E+01	1.1569E+02	1.4988E+02	4.3682E+01	1.9357E+02
7500.0	0.201	3.2723E+01	1.2996E+02	1.6268E+02	5.8488E+01	2.2117E+02
7562.5	0.184	3.1064E+01	1.3774E+02	1.6880E+02	6.9345E+01	2.3815E+02

TABLE VI: PARTIAL PRESSURES (MPA) ABOVE PUN, N/PU= 0.820

TEMP	X(GAS)	P(PU)	P(PUN)	PSAT	P(N2)	PTOT
3000.0	0.972	4.3422E-02	1.2315E-03	4.4653E-02	1.0940E-04	4.4763E-02
3500.0	0.923	2.9874E-01	2.4763E-02	3.2351E-01	1.6061E-03	3.2511E-01
4000.0	0.850	1.2213E+00	2.1512E-01	1.4364E+00	1.2142E-02	1.4485E+00
4500.0	0.764	3.5045E+00	1.0852E+00	4.5897E+00	6.0664E-02	4.6504E+00
5000.0	0.673	7.8176E+00	3.7919E+00	1.1609E+01	2.3120E-01	1.1841E+01
5500.0	0.585	1.4476E+01	1.0249E+01	2.4725E+01	7.3771E-01	2.5462E+01
6000.0	0.502	2.3235E+01	2.3035E+01	4.6270E+01	2.0771E+00	4.8347E+01
6500.0	0.418	3.2543E+01	4.5246E+01	7.7788E+01	5.4796E+00	8.3268E+01
7000.0	0.330	3.9627E+01	8.0309E+01	1.1994E+02	1.4258E+01	1.3419E+02
7250.0	0.281	4.0557E+01	1.0387E+02	1.4443E+02	2.3654E+01	1.6808E+02
7375.0	0.252	3.9616E+01	1.1748E+02	1.5710E+02	3.1223E+01	1.8832E+02
7437.5	0.236	3.8545E+01	1.2476E+02	1.6331E+02	3.6368E+01	1.9968E+02
7476.6	0.224	3.7484E+01	1.2959E+02	1.6708E+02	4.0385E+01	2.0746E+02

TABLE VII: PARTIAL PRESSURES (MPA) ABOVE PUN, N/PU= 0.790

TEMP	X(GAS)	P(PU)	P(PUN)	PSAT	P(N2)	PTOT
3000.0	0.977	4.9914E-02	1.1909E-03	5.1105E-02	7.6845E-05	5.1182E-02
3500.0	0.935	3.4555E-01	2.3935E-02	3.6949E-01	1.1273E-03	3.7062E-01
4000.0	0.871	1.4077E+00	2.0857E-01	1.6163E+00	8.5348E-03	1.6248E+00
4500.0	0.793	4.0511E+00	1.0556E+00	5.1067E+00	4.2771E-02	5.1495E+00
5000.0	0.710	9.0643E+00	3.7054E+00	1.2770E+01	1.6360E-01	1.2933E+01
5500.0	0.625	1.6792E+01	1.0079E+01	2.6871E+01	5.2626E-01	2.7398E+01
6000.0	0.542	2.7003E+01	2.2817E+01	4.9820E+01	1.4874E+00	5.1307E+01
6500.0	0.455	3.7791E+01	4.5179E+01	8.2970E+01	3.9613E+00	8.6932E+01
7000.0	0.361	4.5655E+01	8.0935E+01	1.2659E+02	1.0476E+01	1.3707E+02
7250.0	0.304	4.6080E+01	1.0530E+02	1.5138E+02	1.7692E+01	1.6907E+02
7375.0	0.270	4.4274E+01	1.1945E+02	1.6372E+02	2.3851E+01	1.8757E+02

TABLE VIII: PARTIAL PRESSURES (MPA) ABOVE PUN AT LPB

TEMP	X(GAS)	P(PU)	P(PUN)	PSAT	P(N2)	PTOT
3000.0	0.963	9.3500E-03	1.4400E-03	1.0790E-02	3.3800E-03	1.4170E-02
3500.0	0.963	6.5100E-02	2.8600E-02	9.3700E-02	4.7800E-02	1.4150E-01
4000.0	0.960	2.8400E-01	2.4600E-01	5.3000E-01	2.9500E-01	8.2500E-01
4500.0	0.955	9.0200E-01	1.2120E+00	2.1140E+00	1.2700E+00	3.3840E+00
5000.0	0.948	2.3400E+00	4.1400E+00	6.4800E+00	3.5800E+00	1.0060E+01
5500.0	0.938	5.1200E+00	1.0860E+01	1.5980E+01	7.0000E+00	2.2980E+01
6000.0	0.924	9.9500E+00	2.3800E+01	3.3750E+01	1.3100E+01	4.6850E+01
6500.0	0.904	1.7600E+01	4.5400E+01	6.3000E+01	2.0500E+01	8.3500E+01
7000.0	0.871	2.8900E+01	7.9300E+01	1.0820E+02	2.8600E+01	1.3680E+02
7250.0	0.842	3.4800E+01	1.0300E+02	1.3780E+02	3.3200E+01	1.7100E+02
7375.0	0.816	3.8000E+01	1.1810E+02	1.5610E+02	3.4400E+01	1.9050E+02
7480.0	0.794	3.4600E+01	1.3350E+02	1.6810E+02	3.4700E+01	2.0280E+02

TABLE IX: LIQUID ENTHALTY, LIQUID AND VAPOR DENSITY

TEMP (K)	ENTHALPY (J/MOL)	RHO(LIQ) (G/CM**3)	RHO(VAP) (G/CM**3)
3000.0	53630.0	1.1720E+01	1.1200E-04
4000.0	77823.0	1.0490E+01	4.1000E-03
5000.0	104203.0	9.0300E+00	4.1000E-02
6000.0	134926.0	7.2600E+00	2.0600E-01
6500.0	152933.0	6.2050E+00	4.0200E-01
7000.0	174936.0	4.9270E+00	7.8700E-01
7250.0	189892.0	4.0740E+00	1.1660E+00
7375.0	200920.0	3.4620E+00	1.5320E+00
7480.0	212516.0	2.4000E+00	2.4000E+00

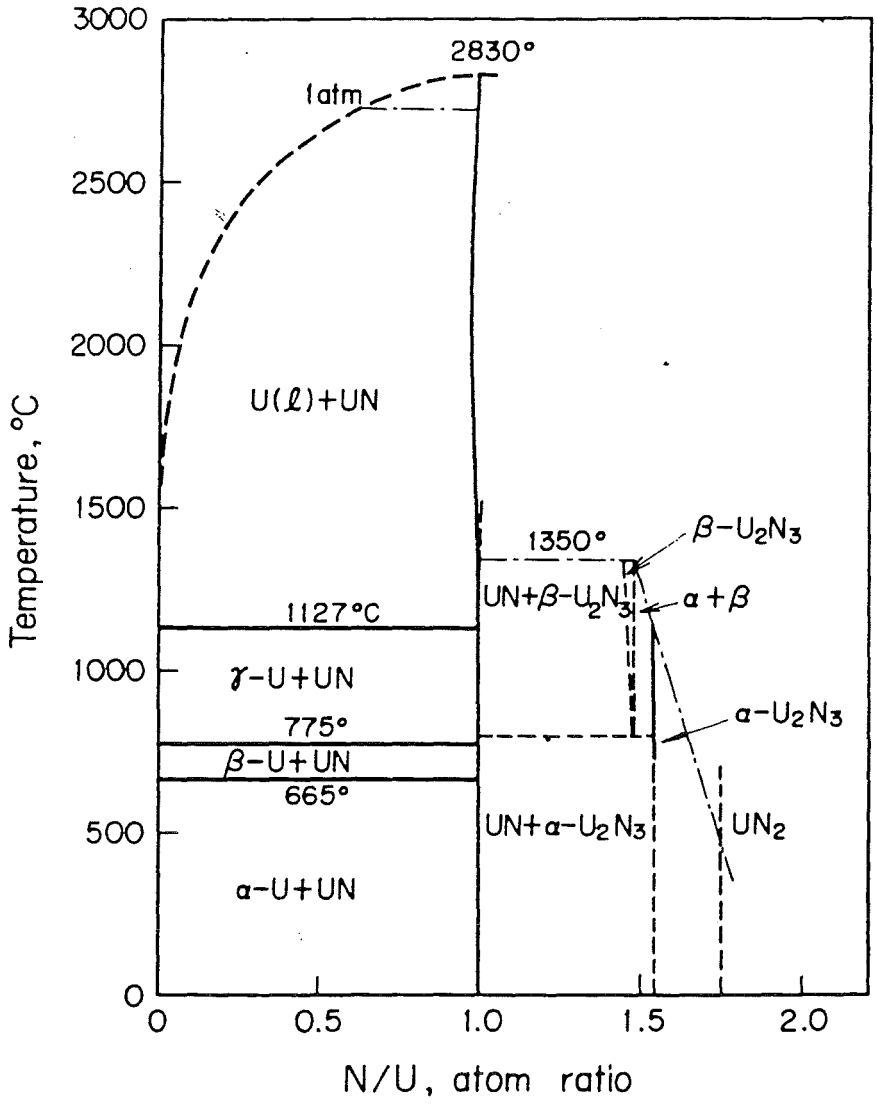

Fig. 1. Phase diagram of the U–N system.

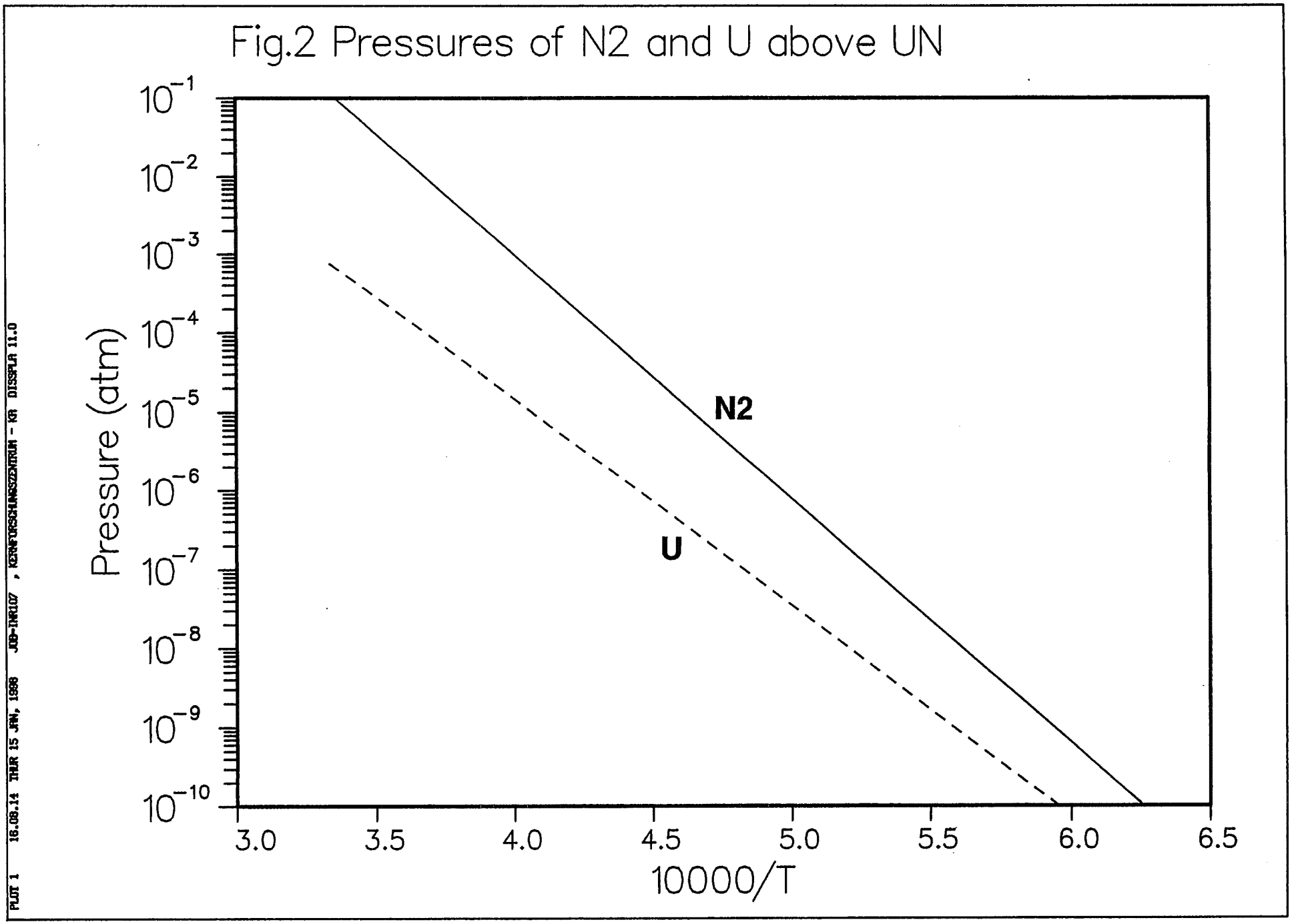
Fig.2 Pressures of N2 and U above UN
Pressure (atm)
10^{-1}
10^{-2}
10^{-3}
10^{-4}
10^{-5}
10^{-6}
10^{-7}
10^{-8}
10^{-9}
10^{-10}
N2
U
3.0
3.5
4.0
4.5
5.0
5.5
6.0
6.5
10000/T
PLOT 1 16.08.14 THUR 15 JAN, 1998 JOB-INR107 , KERNFORSCHUNGSZENTRUM - KR DISSPLA 11.0

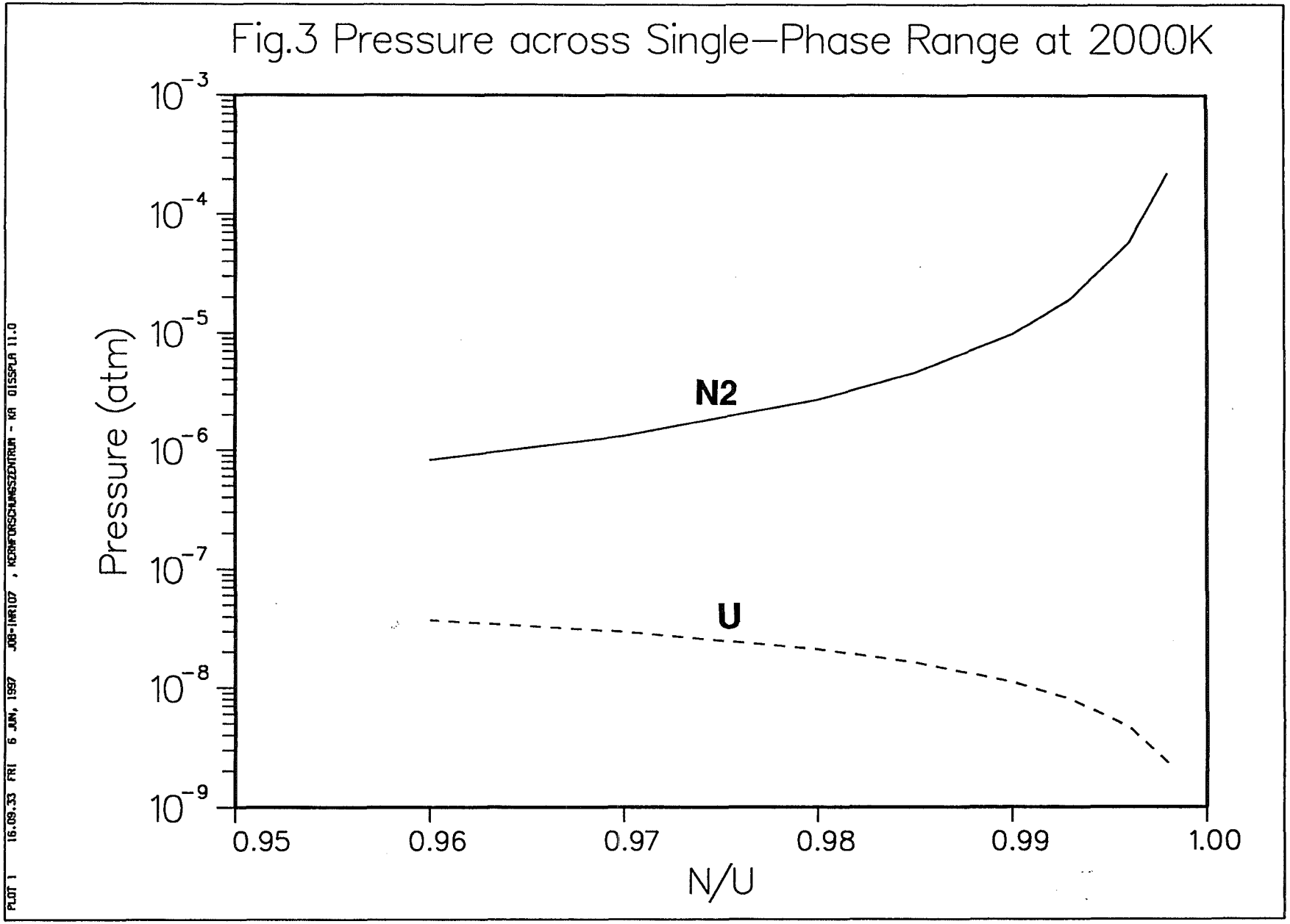
Fig.3 Pressure across Single–Phase Range at 2000K
Pressure (atm)
10^{-3}
10^{-4}
10^{-5}
10^{-6}
10^{-7}
10^{-8}
10^{-9}
N2
U
0.95
0.96
0.97
0.98
0.99
1.00
N/U
PLOT 1 16.09.33 FRI 6 JUN, 1997 JOB=INR107 , KERNFORSCHUNGSZENTRUM - KA GISSPLA 11.0

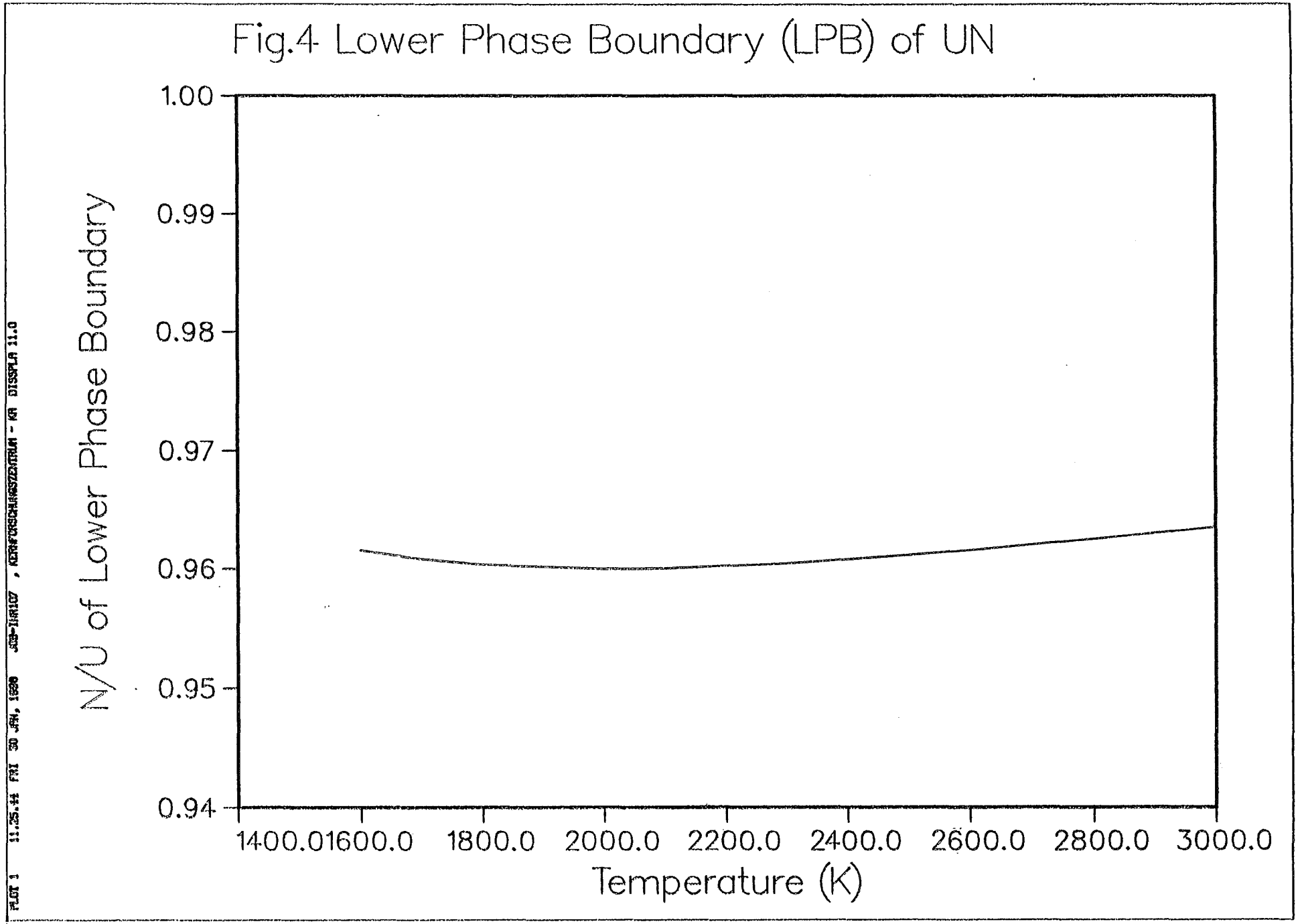
Fig.4 Lower Phase Boundary (LPB) of UN
N/U of Lower Phase Boundary
1.00
0.99
0.98
0.97
0.96
0.95
0.94
1400.0
1600.0
1800.0
2000.0
2200.0
2400.0
2600.0
2800.0
3000.0
Temperature (K)

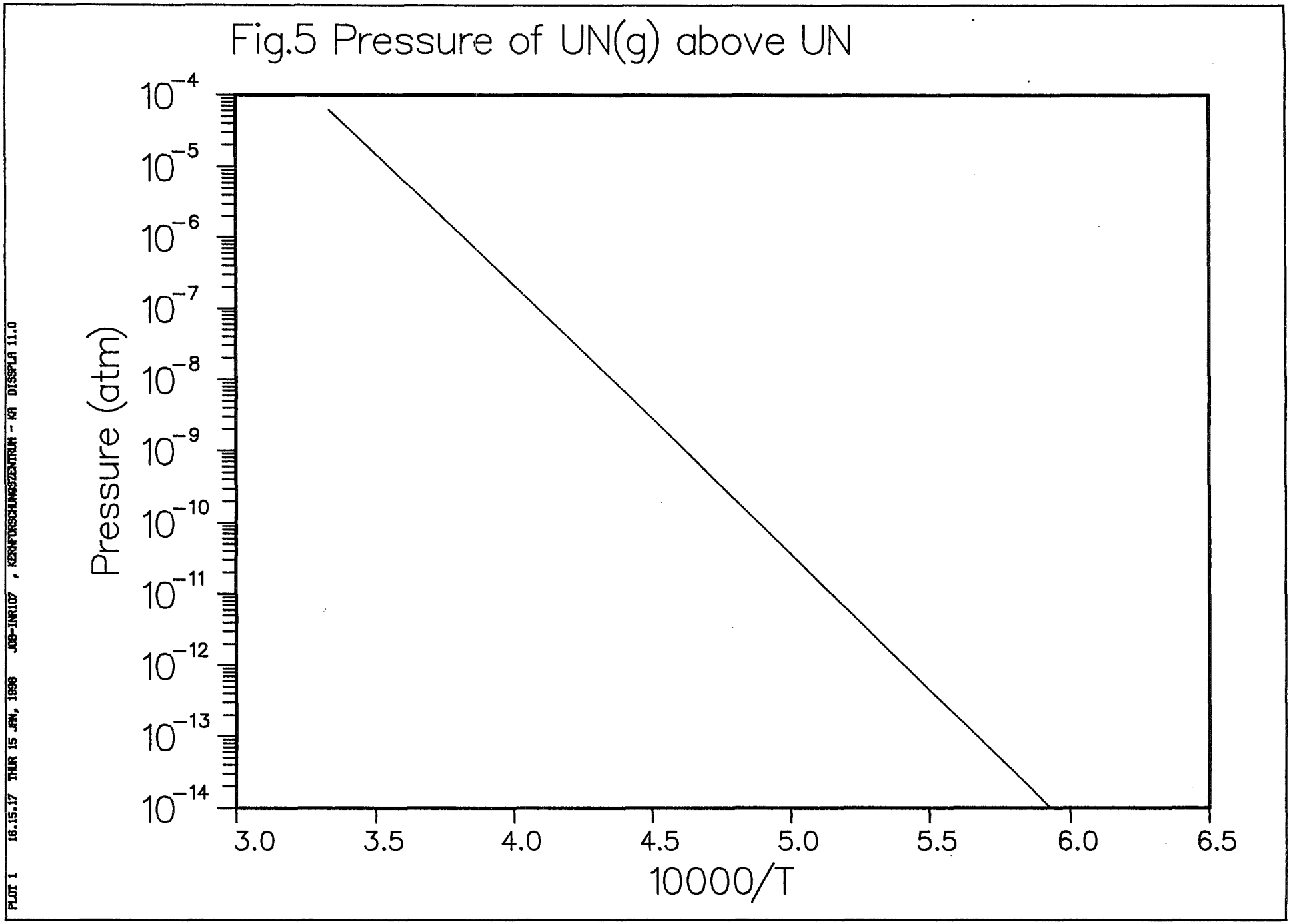
Fig.5 Pressure of UN(g) above UN
Pressure (atm)
10^{-4}
10^{-5}
10^{-6}
10^{-7}
10^{-8}
10^{-9}
10^{-10}
10^{-11}
10^{-12}
10^{-13}
10^{-14}
3.0
3.5
4.0
4.5
5.0
5.5
6.0
6.5
10000/T
PLOT 1 16.15.17 THUR 15 JAN, 1988 JOB-INR107 , KERNFORSCHUNGSZENTRUM - KFI DISSPLA 11.0

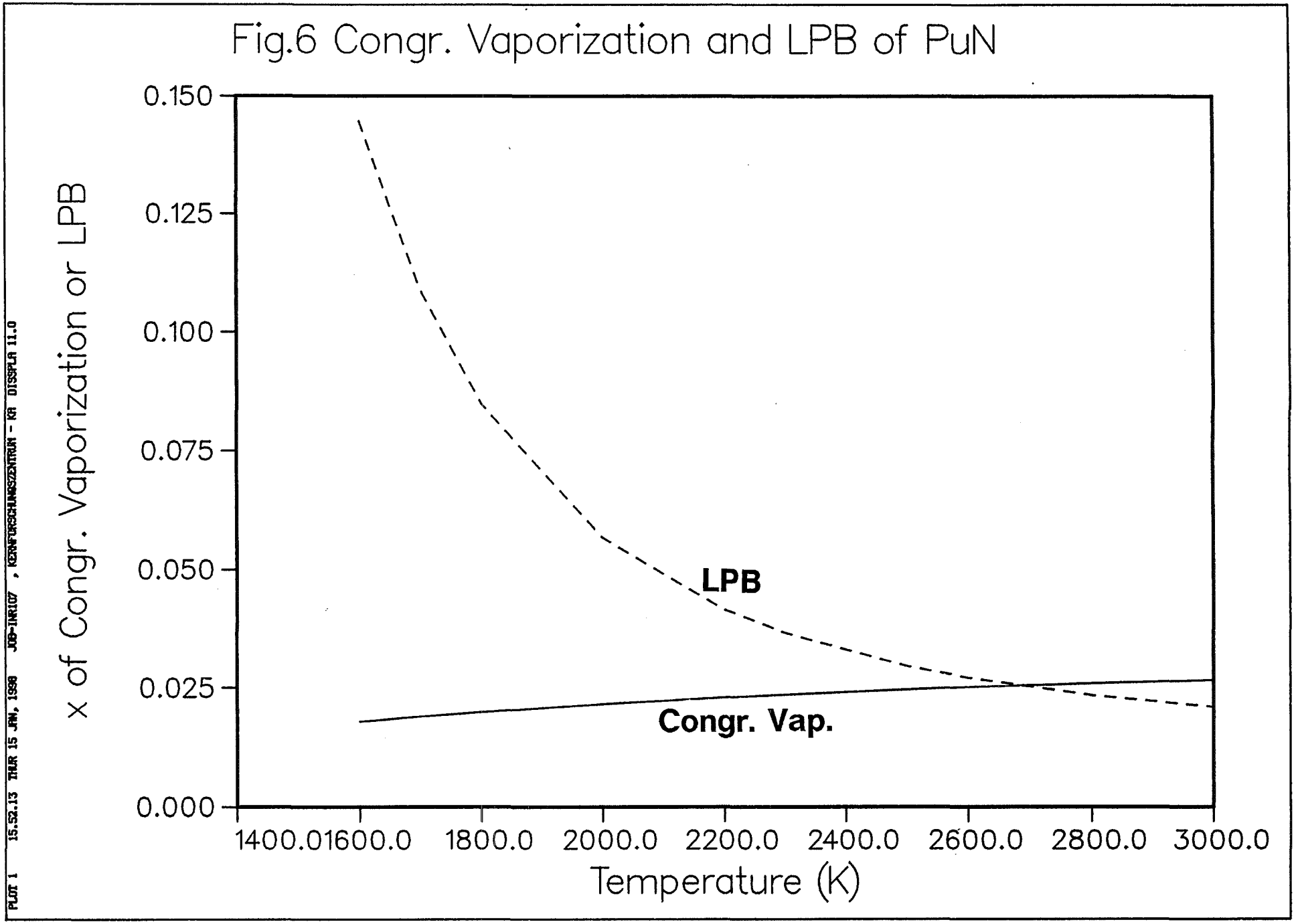
Fig.6 Congr. Vaporization and LPB of PuN
x of Congr. Vaporization or LPB
0.150
0.125
0.100
0.075
0.050
0.025
0.000
LPB
Congr. Vap.
1400.0
1600.0
1800.0
2000.0
2200.0
2400.0
2600.0
2800.0
3000.0
Temperature (K)
PLOT 1 15.52.13 THUR 15 JAN, 1998 JOB-INR107 , KERNFORSCHUNGSZENTRUM - KA DISSPLA 11.0

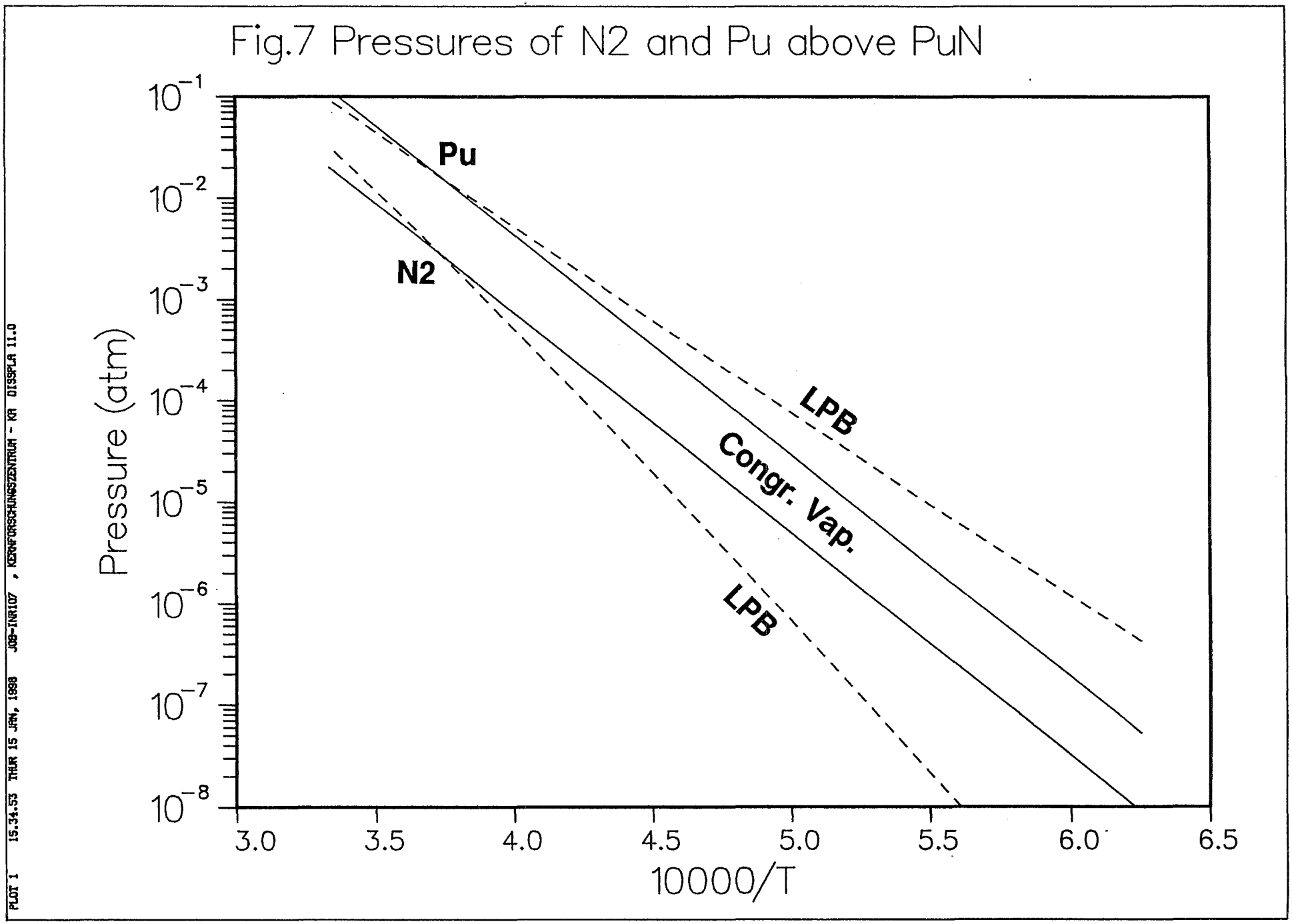
Fig.7 Pressures of N2 and Pu above PuN
Pressure (atm)
10^{-1}
10^{-2}
10^{-3}
10^{-4}
10^{-5}
10^{-6}
10^{-7}
10^{-8}
Pu
N2
LPB
Congr. Vap.
LPB
3.0
3.5
4.0
4.5
5.0
5.5
6.0
6.5
10000/T
PLOT 1 15.34.53 THUR 15 JAN, 1998 JOB=INR107 , KERNFORSCHUNGSZENTRUM - KA DISSPLA 11.0

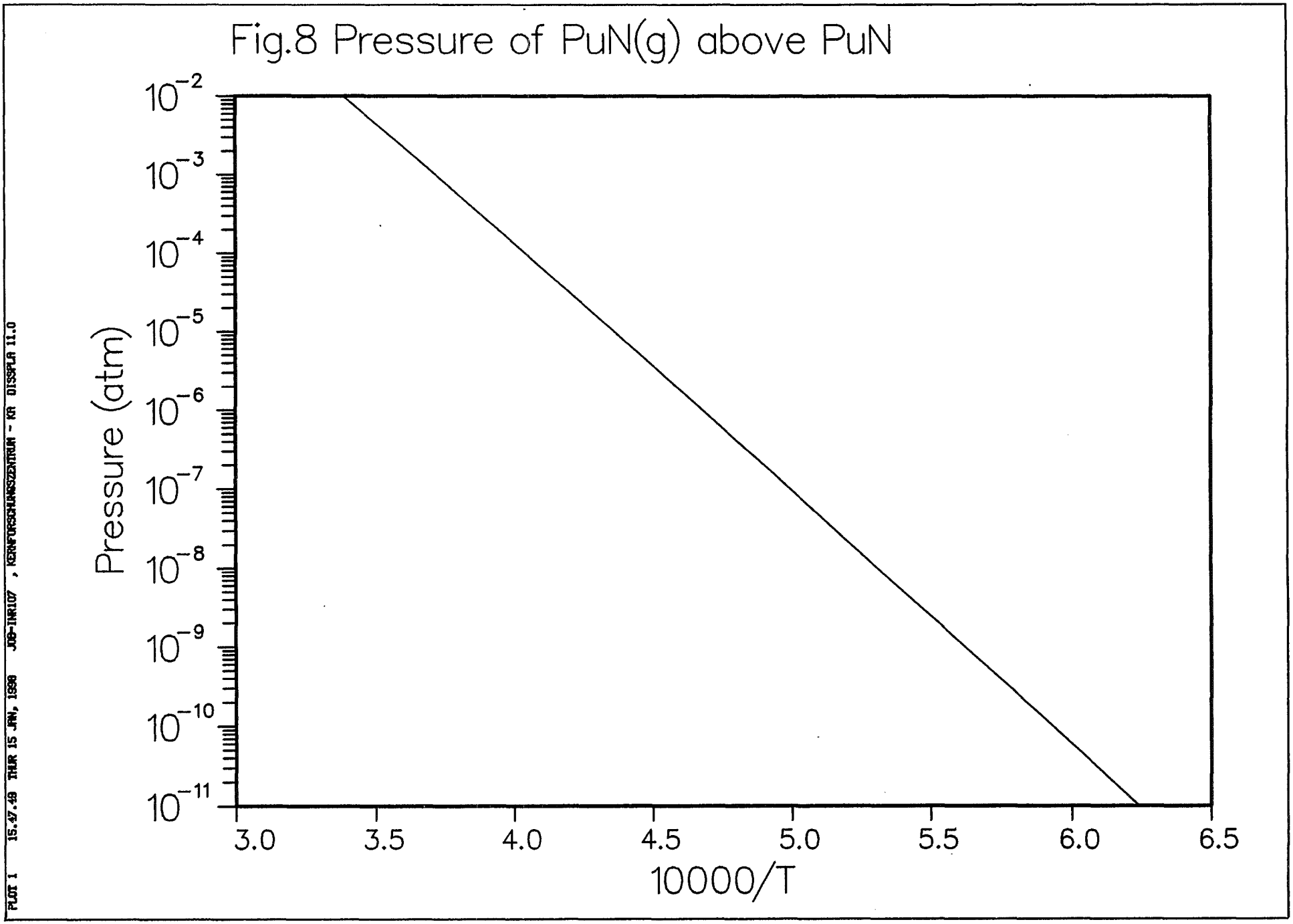
Fig.8 Pressure of PuN(g) above PuN
Pressure (atm)
10^{-2}
10^{-3}
10^{-4}
10^{-5}
10^{-6}
10^{-7}
10^{-8}
10^{-9}
10^{-10}
10^{-11}
3.0
3.5
4.0
4.5
5.0
5.5
6.0
6.5
10000/T
PLOT 1 15.47.49 THUR 15 JAN, 1998 JOB-INR107 , KERNFORSCHUNGSZENTRUM - KA DISSPLA 11.0

Fig.9 Pressures as Function of N/Pu at 2000K

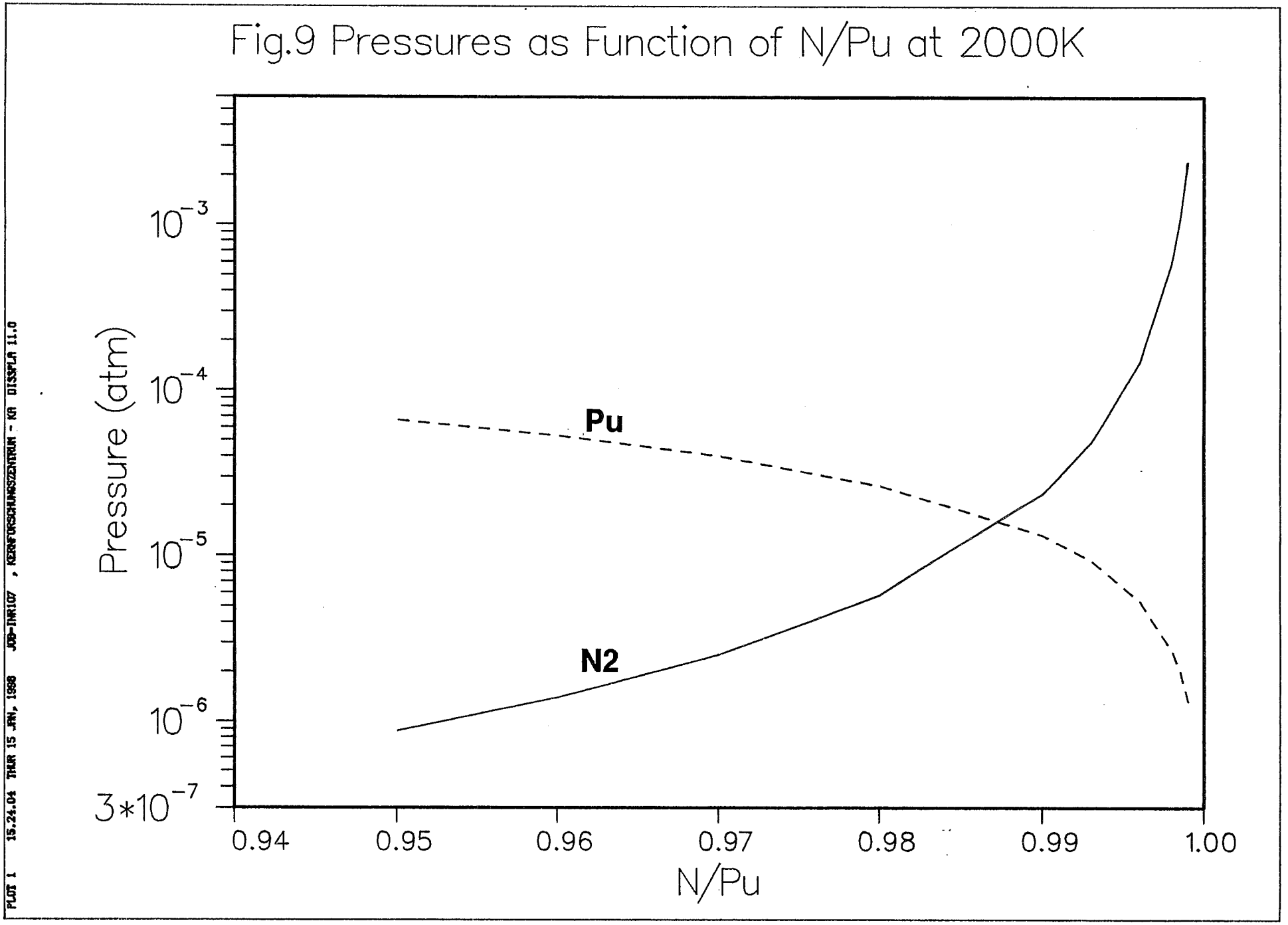

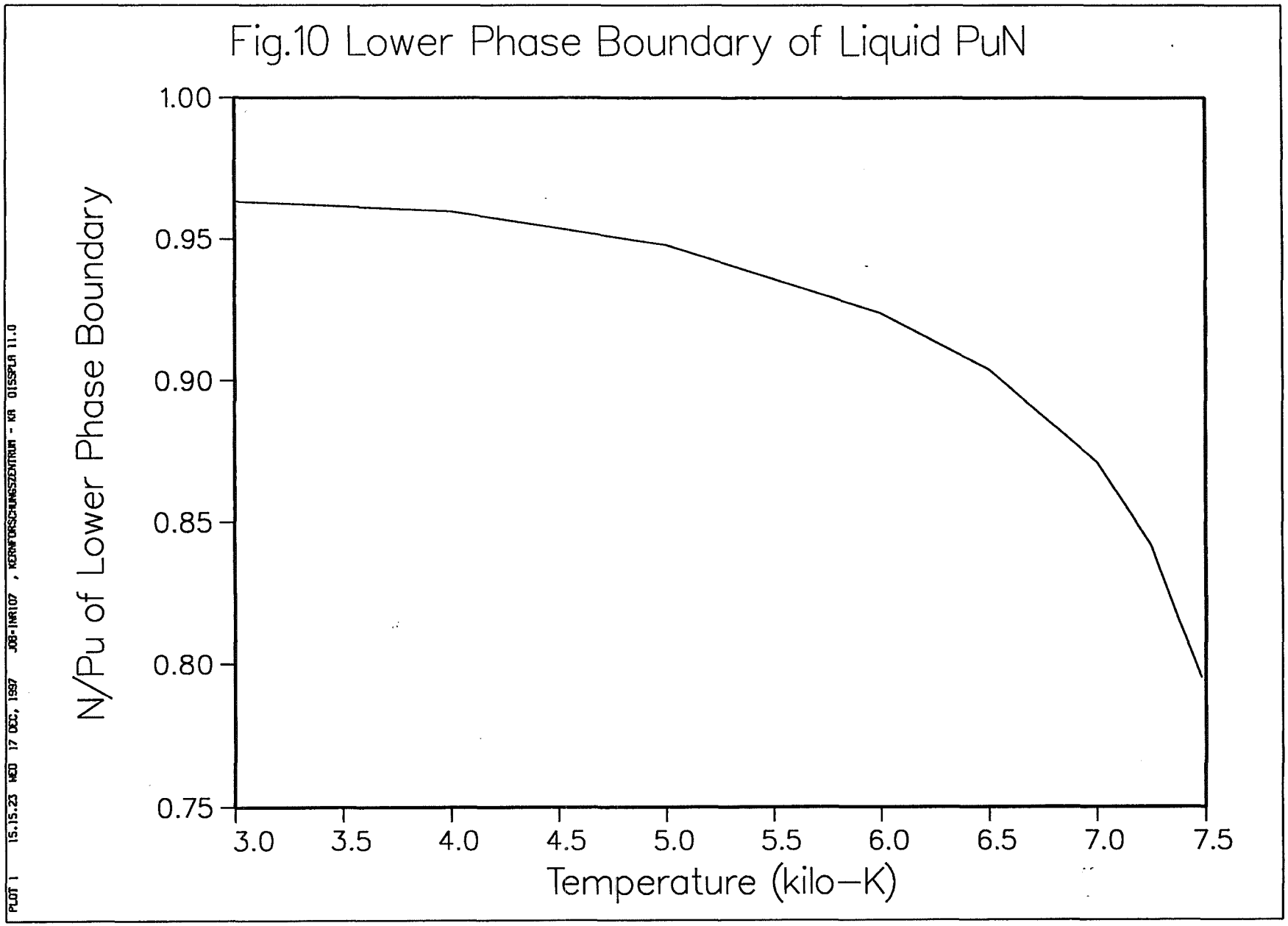
Fig.10 Lower Phase Boundary of Liquid PuN
N/Pu of Lower Phase Boundary
1.00
0.95
0.90
0.85
0.80
0.75
3.0
3.5
4.0
4.5
5.0
5.5
6.0
6.5
7.0
7.5
Temperature (kilo-K)
PLOT 1 15.15.23 MED 17 DEC, 1997 JOB-INR107 , KERNFORSCHUNGSZENTRUM - KA DISSPLA 11.0

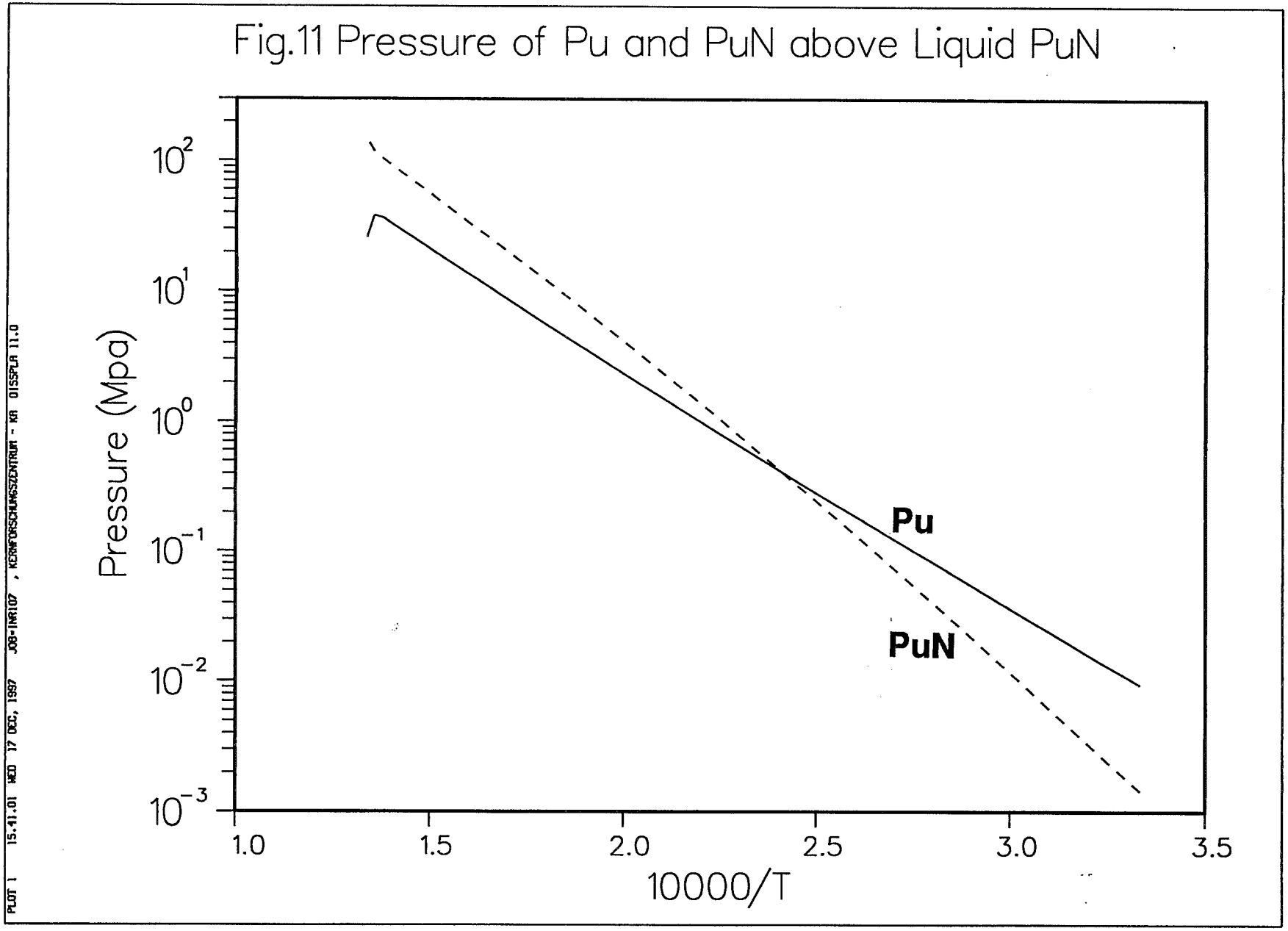
Fig.11 Pressure of Pu and PuN above Liquid PuN
Pressure (Mpa)
10^{2}
10^{1}
10^{0}
10^{-1}
10^{-2}
10^{-3}
1.0
1.5
2.0
2.5
3.0
3.5
10000/T
Pu
PuN
PLOT 1 15.41.01 MED 17 DEC, 1997 JOB-INR107 , KERNFORSCHUNGSZENTRUM - KA DISSPLA 11.0

Fig.12 Saturation and Total Pressure Above PuN

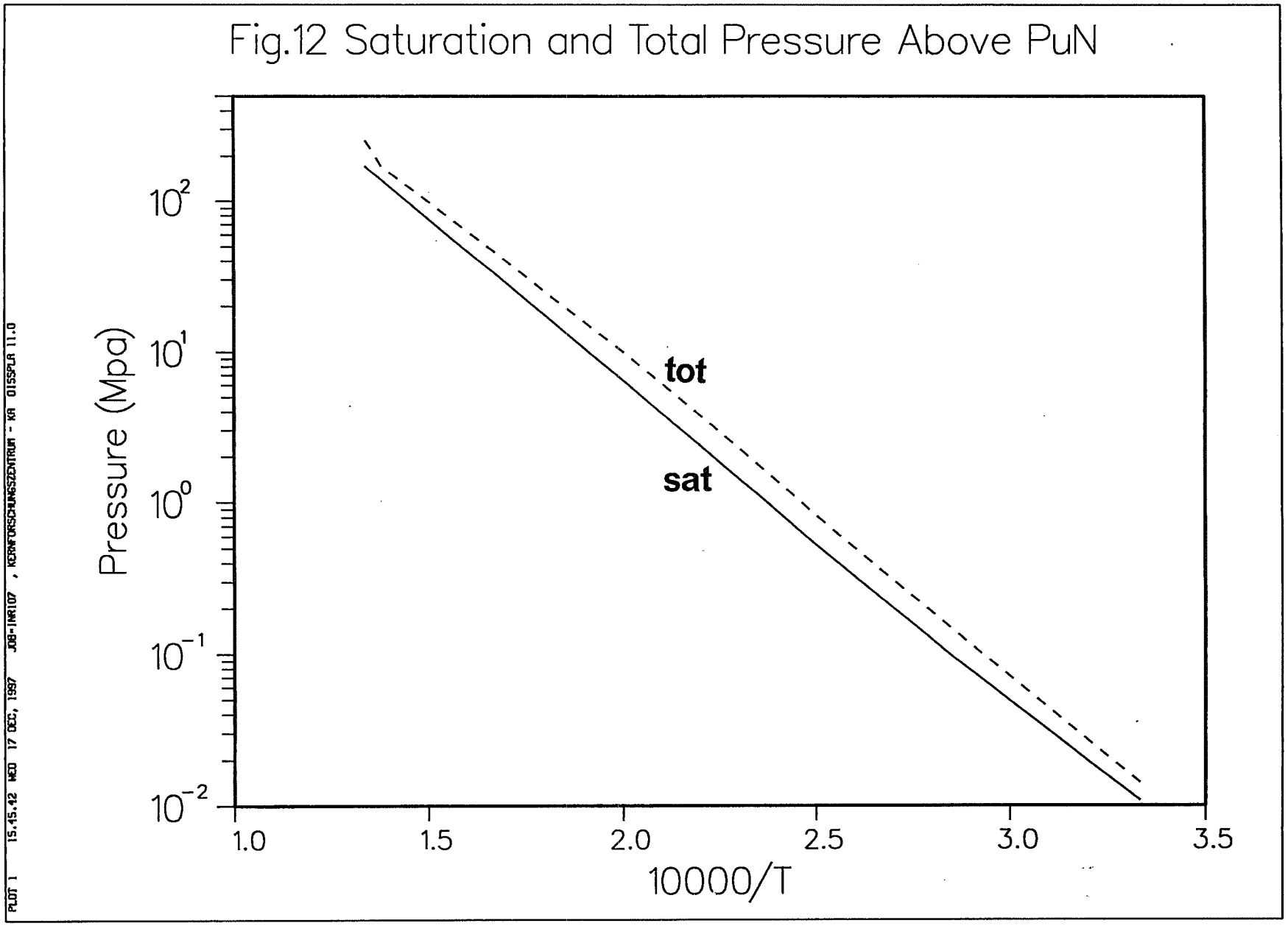

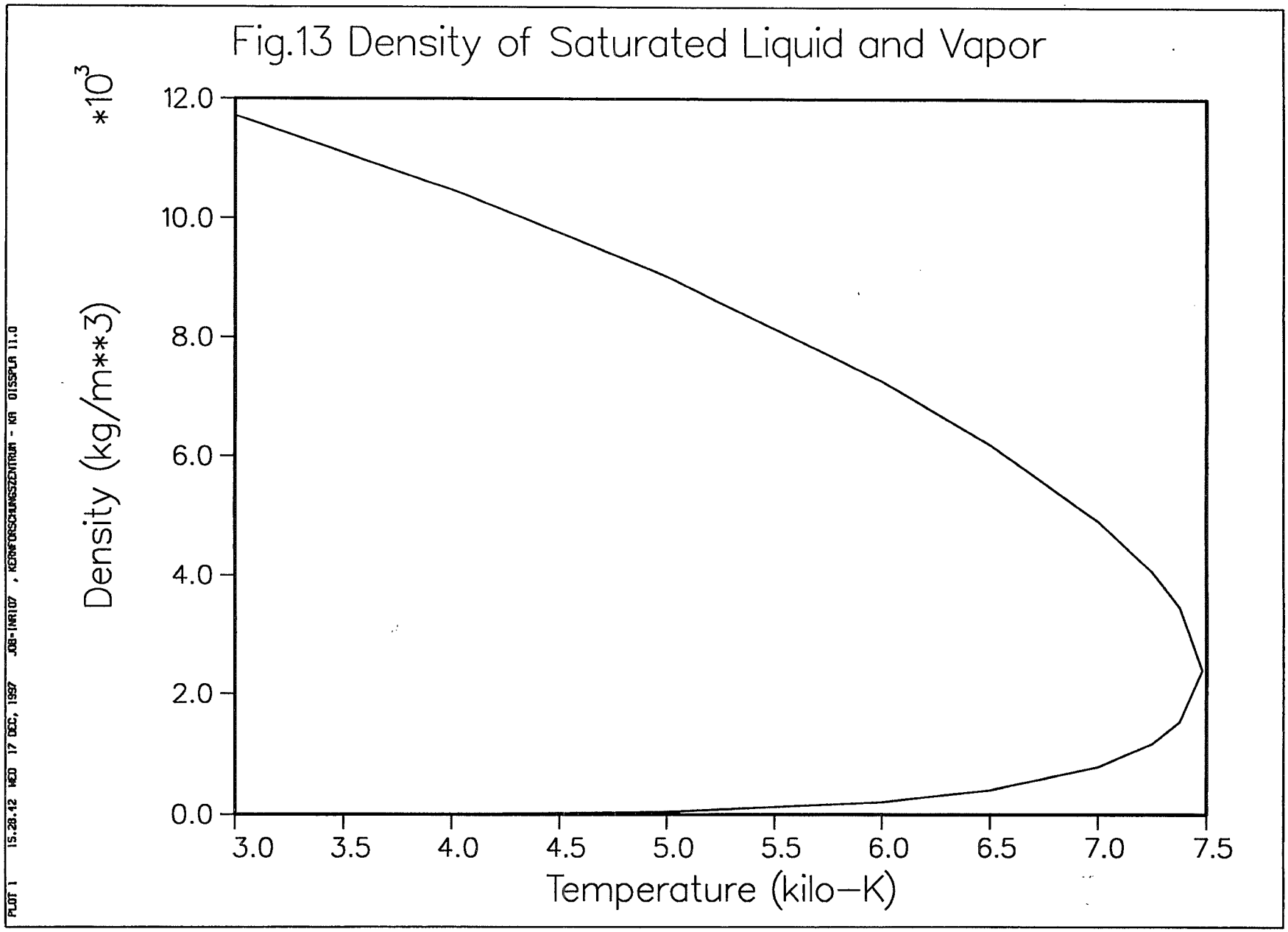
Fig.13 Density of Saturated Liquid and Vapor
Density (kg/m**3)
*10^3
12.0
10.0
8.0
6.0
4.0
2.0
0.0
3.0
3.5
4.0
4.5
5.0
5.5
6.0
6.5
7.0
7.5
Temperature (kilo-K)
PLOT 1 15.28.42 MED 17 DEC, 1997 JOB=NR107 , KERNFORSCHUNGSZENTRUM - KfA DISSPLA 11.0

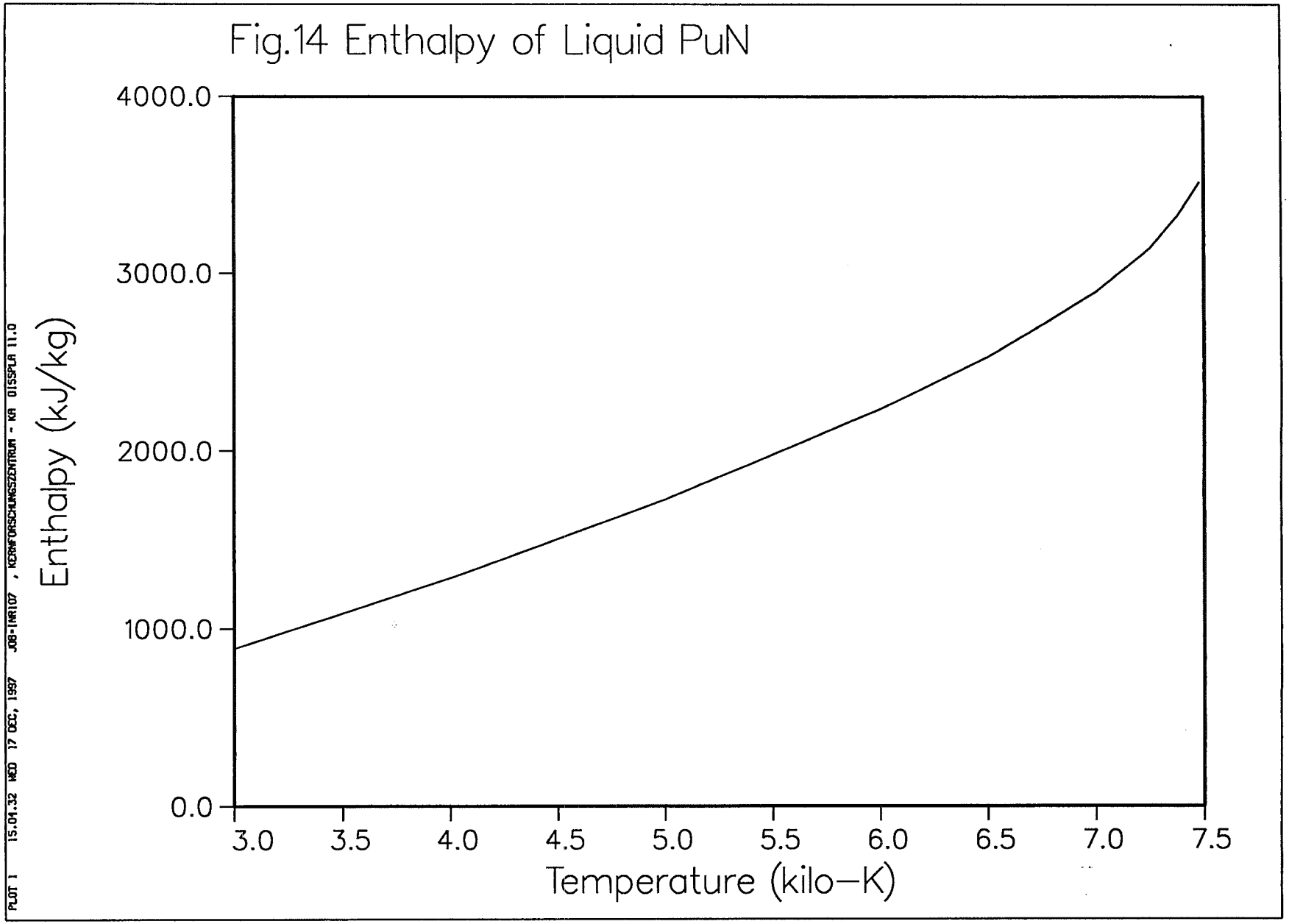
Fig.14 Enthalpy of Liquid PuN
4000.0
3000.0
2000.0
1000.0
0.0
Enthalpy (kJ/kg)
3.0
3.5
4.0
4.5
5.0
5.5
6.0
6.5
7.0
7.5
Temperature (kilo-K)
PLOT 1 15.04.32 MED 17 DEC, 1997 JOB-INR107 , KERNFORSCHUNGSZENTRUM - KA DISSPLA 11.0